

December 2013

Steady-State Voltage Security Assessment Using Symmetric Eigenvalue Analysis for Weak Area Identification in Large Power Transmission Network

Yagnaramasubramanian Somayajulu
University of Wisconsin-Milwaukee

Follow this and additional works at: <https://dc.uwm.edu/etd>



Part of the [Electrical and Electronics Commons](#)

Recommended Citation

Somayajulu, Yagnaramasubramanian, "Steady-State Voltage Security Assessment Using Symmetric Eigenvalue Analysis for Weak Area Identification in Large Power Transmission Network" (2013). *Theses and Dissertations*. 310.
<https://dc.uwm.edu/etd/310>

This Thesis is brought to you for free and open access by UWM Digital Commons. It has been accepted for inclusion in Theses and Dissertations by an authorized administrator of UWM Digital Commons. For more information, please contact open-access@uwm.edu.

STEADY-STATE VOLTAGE SECURITY ASSESSMENT USING
SYMMETRIC EIGENVALUE ANALYSIS FOR WEAK AREA
IDENTIFICATION IN LARGE POWER TRANSMISSION NETWORK

by

Yagnaramasubramanian Somayajulu

A Thesis Submitted in

Partial Fulfillment of the

Requirements for the Degree of

Master of Science

in Engineering

at

The University of Wisconsin-Milwaukee

December 2013

ABSTRACT

STEADY-STATE VOLTAGE SECURITY ASSESSMENT USING SYMMETRIC EIGENVALUE ANALYSIS FOR WEAK AREA IDENTIFICATION IN LARGE POWER TRANSMISSION NETWORK

by

Yagnaramasubramanian Somayajulu

The University of Wisconsin-Milwaukee, 2013
Under the Supervision of Professor David C. Yu

The central focus of this thesis is on long-term static voltage stability analysis of large power transmission grid. This thesis work is a product of an attempt to comprehend the numerous researches that has been done over the years on voltage security assessment. Voltage stability is one of the essential components influencing the reliability of a power network. There are several Transmission planning and operation compliance standards pertaining to voltage criterion from NERC and Independent System Operators (ISO) directed toward the utilities to operate their grid within tight voltage limits. This requires the utility to perform comprehensive planning studies of the power system frequently for different load profiles like summer and winter - peak load and light load conditions taking into account several contingency scenarios. The humongous number of nodes and branches in a typical preset-day power network has increased the complexity of conventional voltage stability analysis methods like PV / QV curves.

Initially, this study discusses various linear algebraic techniques used in steady-state power system analysis and presents the results on the simulations of IEEE test systems – 14 bus, 30 bus and 118 bus system. Later, it introduces an idea of performing a spectral (Symmetric Eigenvalue) analysis of the power system Jacobian and a rigorous testing of the same IEEE bus test systems was performed. Finally, it concludes by presenting a comparative result against other eigenvalue-based methods. The entire analysis has been performed by a combination of custom-written MATLAB programs, Python scripts and Siemens PTI PSS/E software for its one-line diagram capabilities.

© Copyright by Yagnaramasubramanian Somayajulu, 2013
All Rights Reserved

Dedicated to my parents

TABLE OF CONTENTS

1. INTRODUCTION	1
1.1. Definitions of Stability.....	2
1.2. Types of Disturbances.....	2
1.3. Time frame of study:.....	3
1.4. Importance of Voltage Stability Analysis.....	3
1.5. Voltage Stability versus Voltage Security	4
1.6. Overview of Methodology	5
2. DISCUSSION OF CONVENTIONAL VOLTAGE STABILITY ANALYSIS METHODS .	6
2.1. PV/QV Curves	6
2.2. Minimum Singular Value Technique.....	8
2.3. Reduced Jacobian Modal Analysis Method.....	8
3. SYMMETRIC EIGENVALUE ANALYSIS – PROPOSED METHOD	10
3.1. Breakdown into Symmetric and Asymmetric Jacobian Matrices	10
3.2. Formulation of Voltage Stability Indices from J_S and J_{AS}	11
3.3. GERSHGORIN CIRCLE THEOREMS	15
3.3.1. Application of Gershgorin circle theorem to IEEE test systems.....	16
3.4. Modal Analysis of Symmetric Jacobian Matrix	19
3.4.1. IEEE 14-bus test system	19
3.4.2. IEEE 30-bus test system	22
3.4.3. IEEE 118-bus test system	27
4. FUTURE WORK.....	34
4.1. Simulation on the entire eastern interconnection.....	34
5. CONCLUSION.....	40
6. REFERENCES	41
APPENDICES: MATLAB PROGRAMS	42
Appendix A. Admittance matrix calculation:	42
Appendix B. Custom Load flow program – Individual Bus Investigation	43
Appendix C. Custom Load flow program – Critical Mode Identification.....	49
Appendix D. Solution and Results Program	54
Appendix E. Jacobian Indices and Gerschgorin Circles	56

LIST OF FIGURES

Figure 1. Example of PV Curve.....	7
Figure 2. . Jacobian Indices on IEEE 14-bus	14
Figure 3. Jacobian Indices on IEEE 30-bus	14
Figure 4. Jacobian Indices on IEEE 118-bus	15
Figure 5. . Gershgorin circle plot for IEEE 14-bus system.....	17
Figure 6. Gershgorin circle plot for IEEE 30-bus system.....	18
Figure 7. Gershgorin circle plot for IEEE 118-bus system.....	18
Figure 8. One line diagram - IEEE 14-bus test system.....	20
Figure 9. Mode Shape – IEEE 14-Bus system.....	21
Figure 10. Participation factors – IEEE 14-Bus system	22
Figure 11. PV curves – IEEE 14-bus system.....	22
Figure 12. One line diagram - IEEE 30 Bus system.....	23
Figure 13. Mode Shape - IEEE 30 Bus system.....	25
Figure 14. Bus Participation Factors - IEEE 30 Bus system	25
Figure 15. Bus Participation factors zoomed in by a factor of 1000 - IEEE 30 Bus system	26
Figure 16. PV Curves - IEEE 30 Bus system	26
Figure 17. One-line diagram of IEEE 118-Bus system	28
Figure 18. Mode Shape – IEEE 118 Bus system	32
Figure 19. Bus Participation Factors – IEEE 118 Bus system.....	32
Figure 20. Bus Participation Factors scaled by a factor of 10000 – IEEE 118 Bus system	33
Figure 21. PV Curves of critical buses – IEEE 118 Bus system	33

Figure 22. Three-dimensional plot with coherent groups forming distinct areas	38
Figure 23. Angular Plot of Group 1	38
Figure 24. Angular Plot of Group 2 Angular Plot of Group 2.....	39
Figure 25. Angular Plot of Group 3	39
Figure 26. Angular Plot of Group 4.....	39

LIST OF TABLES

Table 1. List of Indices and their expressions.....	12
Table 2. Load and generation profile for IEEE 14-bus system.....	20
Table 3. Load and generation profile for IEEE 30-bus system.....	24
Table 4. Load and generation profile for IEEE 118-bus system.....	28
Table 5. Correlation Matrix – From time-stamped angle data.....	36
Table 6. Most Significant Principal Components.....	37

ACKNOWLEDGEMENTS

I would like to express my sincerest thanks to Professor Yu for believing in me since the day I pitched in my research idea and providing me with guidance and also offering me the financial support. Without his encouragement and timely response to all my questions, this thesis work would not have been completed in time.

I owe a special thanks to my colleague at National Grid, Dr. Per-Anders Löf for generously sharing his knowledge on voltage stability and offering me his doctoral thesis work for my reference. It had helped me comprehend certain facts that were unanswered during the crucial period of my research.

I would also like to thank all my colleagues from research group and special thanks to Ashish Solanki for being supportive during the initial stages of my graduate studies and getting me acquainted with the fundamentals of power systems research.

1. INTRODUCTION

Voltage instability is a phenomenon that causes the electric power grid to fail due to a collapsing voltage which penetrates across the power network. Voltage stability is a well understood concept thanks to the numerous researches over the past few decades but still the challenges exist, including formulating ways to effectively manage the electric power grid to avert such events, or to stop it quickly and effectively when it occurs. Considering the topic of voltage security, it is rather unavoidable to not to mention about the blackouts. Several blackout incidents that took place over last few decades have been victim to the voltage stability issues in the power grid. A blackout in an electric system means that the complete system collapses and affects all utility consumers in the area. It can originate from several causes. One of the prominent causes is an overload of the transmission system caused by congestion, forcing an overloaded transmission line to trip, causing increased loading of other lines which in turn results in additional trips, and, in the end – a voltage collapse due to the high impedance in the weakened power network. Thus cascading failures of several transmission lines result in a system-wide blackout while the root-cause being the system operating very close to its capacity. Few examples of significant blackout incidents are Germany in 2006 and Russia in 2005, in Greece 2004, Italy in 2003 and in the same year, blackouts occurred in USA and Canada, Sweden-East Denmark, London, UK and Croatia and Bosnia-Herzegovina and most recently, India in July 2012. All these blackouts have been reviewed in detail and results have been well documented by IEEE task forces. ^[1]

Due to this very fact, voltage instability phenomenon has been regarded as a distinct and vital subject for power systems research and development. This chapter will discuss various definitions, background to this thesis research and overview of methods being developed as a part of this work.

1.1. Definitions of Stability

The term, ‘Stability’ have been extensively reviewed and explained by several power systems research organizations like IEEE, CIGRE, EPRI, etc. Since this research is focused on steady-state voltage stability, it is important to put forth the definitions of important types of stability to avoid any spurious assumptions.^[2]

- (a) *Static Stability*: It denotes the general mathematical term for study of systems of algebraic equations and quasi-static disturbances.
- (b) *Dynamic Stability*: It denotes the general mathematical term for study of systems of differential equations and random and large time-varying disturbances
- (c) *Steady-state Stability*: It denotes the study of power system stability in steady-state, except for the influence of slow and small disturbances.
- (d) *Transient Stability*: It denotes the study of power system stability under the influence of highly disturbed state; in particular its ability to restore or find an operating point acceptably close to the initial one after a large disturbance event.

1.2. Types of Disturbances

To determine the type of voltage stability in consideration for this research viz. steady-state and transient, it is importance to discuss the two types of disturbances:

- (a) *Small disturbance*: It refers to the disturbance for which equations that describes the dynamics of the power system may be linearized for the purpose of analysis.
- (b) *Large disturbance*: It refers to the disturbance for which the equations that describe the dynamics of the power system cannot be linearized for the purpose of analysis.

1.3. Time frame of study:

- (a) *Short-term stability*: A power system is stable in the short-term if it is found to be stable when the study of its behavior is limited to several seconds.
- (b) *Long-term stability*: A power system is stable in the long-term if it found to be stable when the study of its behavior is extended beyond several seconds.

From the above definitions, we can derive the definition of steady-state stability as, for a particular operating point, if following any small disturbance, it reaches a steady-state operating condition that is identical or close to the pre-disturbance operating condition. Thus, it is now clear that this thesis work can be categorized as a study of long-term steady-state voltage stability.

1.4. Importance of Voltage Stability Analysis

Amongst other stability issues like rotor angle and frequency stability, voltage stability is deemed to be the most important and critical in modern-day power network. The long-term voltage stability cannot be fully analyzed by the use of transient angular stability because of the fact that during the final stages of grid collapse, the phenomenon of angle and voltage instability are deeply associated and when the system collapses,

there are a number of concurrently occurring events. It is known fact that voltage stability largely depends on the capability of the power system to provide reactive power support and it has to be locally available. Thus, in the event of grid collapse, the transmission system is affected the most by voltage instability due to the lack of reactive power support. This problem has rather become more obvious in the present-day scenario with the growing complexity of power network.

1.5. Voltage Stability versus Voltage Security

The following definitions from IEEE Power Engineering Society best describe the difference between the terms ‘stability’ and ‘security’.

- (a) *Voltage Stability*: It is the ability of the system to maintain voltage so that when load admittance is increased, the load power will increase so that both voltage and power are controllable.
- (b) *Voltage security*: It is the ability of the power system, not only to operate stably but to remain stable following any reasonably credible contingency or adverse system change.

Thus, from the above definition, it is realized that to successfully alleviate system-wide blackout which occurs as a result of a “Domino Effect” of tripping transmission lines, the voltage stability has to be studied taking into consideration several possible contingency scenarios. So, it is essential to perform voltage security analysis as “security” is a more stringent measure than “stability”.

1.6. Overview of Methodology

It is to be noted that only static aspects of long-term voltage stability issues have been studied based on power flow computations, aimed at determining the voltage stability margins. On reviewing several literatures on voltage stability analysis, it is realized that a common opinion on voltage stability is modal analysis of Reduced Jacobian matrix. Compared with the conventional PV/QV curve methods where the voltage magnitude at the nodes is plotted against changes in the active power injections, the use of eigenvalue analysis technique will attempt to determine both the distance to voltage collapse and the mechanisms of voltage instability.^[3] Due to the high non-linearity of the power system in the vicinity of nose point region, the eigenvalue decomposition of the Jacobian matrix becomes less accurate or in some cases erroneous. To overcome this issue, the thesis work explores the idea of using approximate expression of Jacobian matrix, based on the degree of symmetricity of the matrix, into the conventional reduced eigenvalue decomposition method. Thus, by utilizing various properties of a symmetric eigenvalue decomposition (spectral decomposition), a better prediction of voltage collapse margin is identified. This thesis consists of primarily four parts: Discussion of conventional voltage stability analysis methods, Formulation and simulation of symmetric eigenvalue decomposition techniques, Comparative results and verification section and Future work.

2. DISCUSSION OF CONVENTIONAL VOLTAGE STABILITY

ANALYSIS METHODS

2.1. PV/QV Curves

The PV/QV curves illustrate the variation of voltage with respect to the variation of P and Q components of the load power. These curves are plotted by simulating the load flow solution at several points of increasing load factors until the power flow solution diverges; by maintain a constant power factor. Since the conventional Newton-Raphson method cannot solve near the voltage collapse scenarios, continuation algorithm is generally used to plot the curve beyond the voltage collapse point. The purpose of continuous load flows is to find a set of load flow solutions in a scenario where the load is continuously changing, starting from a base case until the critical point. Thereafter, the continuous load flows had been applied to understand and evaluate the problem of voltage stability and those areas that are likely to the voltage collapse. Besides, they have also been applied in other related problems like the evaluation of power transfer limits between regions. The general principle of continuous load flows employs a predictor-corrector scheme to find a trajectory of solutions for the set of load flow equations which are reformulated to include the load parameter λ .^[4] The process is started from a known solution and a predictor vector which is tangent to the corrected solutions is used to estimate the future solutions with different values of the load parameter. The estimation is

corrected using the same technique of the Newton-Rhapson employed in the conventional load flow with a new added parameter:

$$\mathbf{f}(\theta, \mathbf{V}, \lambda) = \mathbf{0}$$

This parameterization plays an important role in the elimination of the Jacobian non-singularity. In a nutshell, Continuation power flow method can be used to trace the path of a power system from a steady state equilibrium point to a bifurcation point according to the load increase. In this method, we can move along the bifurcation path by taking the following two steps: Predictor step realized by the computation of the tangent vector and corrector step that can be obtained by perpendicular intersection. Figure 1 portrays an example of a complete PV curve.

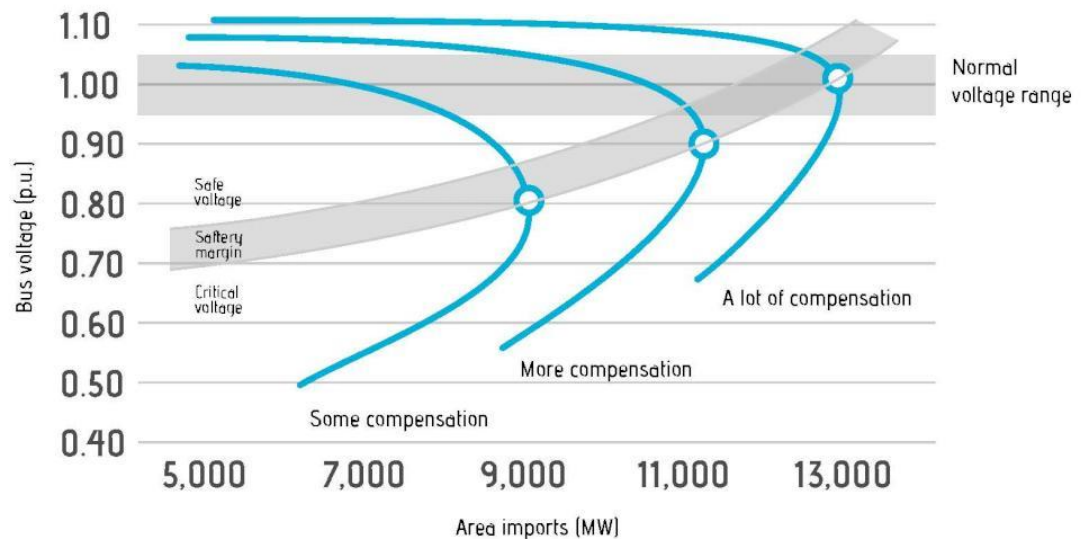


Figure 1. Example of PV Curve

Although PV curves are good indicators of voltage magnitudes at each nodes or buses, it may be a good tool to study the effects of shunt capacitor compensation at individual buses. But, from a system-wide perspective, voltage magnitudes at nodes, alone, do not

constitute reliable indicators of the proximity of the system to the steady-state voltage stability limit. In reality, decisions on reactive power compensation made per the PV curves may hide the imminent close-to-stability limit operating conditions by showing misleading voltage magnitudes in the study area.

2.2. Minimum Singular Value Technique

In this method, a singular value decomposition of the Jacobian matrix is performed at a stable operating point and the minimum singular value is used as a stability index to determine the distance from the operating point to the point of voltage collapse. ^[5]

Although, it is successful in finding a valid stability indicator, it cannot find the cause of the voltage collapse since it is only a relative measure of the system to instability. This technique can only be starting point or a supporting method to the conventional PV/QV analysis to determine the actual stability margin.

2.3. Reduced Jacobian Modal Analysis Method

In this method, an eigenvalue decomposition of a reduced Jacobian matrix, J_R is performed to determine both the proximity index and the cause or mechanisms of voltage instability. ^[6] Since the voltage variation is affected the most by reactive power and in a stable operating point, it is assumed that the real power P is constant. The equations below represent the conventional load flow equation as a function of real and reactive power.

$$P_k = \sum_{j=1}^N |V_k| |V_j| (G_{kj} \cos(\theta_k - \theta_j) + B_{kj} \sin(\theta_k - \theta_j)), \quad k = 2, \dots, N$$

$$Q_k = \sum_{j=1}^N |V_k| |V_j| (G_{kj} \sin(\theta_k - \theta_j) - B_{kj} \cos(\theta_k - \theta_j)), \quad k = N_G + 1, \dots, N$$

By applying Taylor series expansion to the above equations, the Jacobian matrix equation is derived as,

$$\begin{bmatrix} \underline{J}^{P\theta} & \underline{J}^{PV} \\ \underline{J}^{Q\theta} & \underline{J}^{QV} \end{bmatrix} \begin{bmatrix} \underline{\Delta\theta} \\ \underline{\Delta|V|} \end{bmatrix} = - \begin{bmatrix} \underline{\Delta P} \\ \underline{\Delta Q} \end{bmatrix}$$

Where,

$$J_{jk}^{P\theta} = \frac{\partial P_j}{\partial \theta_k} \quad J_{jk}^{Q\theta} = \frac{\partial Q_j}{\partial \theta_k} \quad J_{jk}^{PV} = \frac{\partial P_j}{\partial |V_k|} \quad J_{jk}^{QV} = \frac{\partial Q_j}{\partial |V_k|}$$

In the above equation, when $\underline{\Delta P} = 0$, then the reduced Jacobian matrix, \mathbf{J}_R is derived as,

$$\begin{bmatrix} 0 \\ \underline{\Delta Q} \end{bmatrix} \begin{bmatrix} \underline{J}^{P\theta} & \underline{J}^{PV} \\ \underline{J}^{Q\theta} & \underline{J}^{QV} \end{bmatrix} = \begin{bmatrix} \underline{\Delta\theta} \\ \underline{\Delta|V|} \end{bmatrix} \quad \text{Hence, } \underline{J}_R = [\underline{J}^{QV} - \underline{J}^{Q\theta} \underline{J}^{P\theta^{-1}} \underline{J}^{PV}]$$

From the reduced Jacobian matrix expression, the modes of the power system can be determined from its eigenvalues and eigenvectors.

$$\mathbf{J}_R = \Phi \Lambda \Gamma$$

If all eigenvalues of the reduced Jacobian matrix are positive, the system is voltage stable. A zero eigenvalue means that the system is on the border of voltage collapse and the smallest magnitude of eigenvalue of the reduced Jacobian matrix determines the critical bus or weakest bus in a power system.

By inverting \mathbf{J}_R matrix to \mathbf{J}_R^{-1} , we get

$$\mathbf{J}_R^{-1} = \Phi \Lambda^{-1} \Gamma$$

If Φ_i and Γ_i represent the right- and left- hand eigenvectors respectively for the eigenvalue λ_i of the matrix \mathbf{J}_R , the participation factor measuring the participation of the k^{th} bus in i^{th} mode is defined as :

$$P_{ki} = \Phi_{ki} \Gamma_{ik}$$

The left and right eigenvectors corresponding to the critical modes are used to identify the buses participating in the critical modes. Thus, the nodes or elements with large participation factors are identified as weak areas of the power grid from the perspective of voltage stability.

3. SYMMETRIC EIGENVALUE ANALYSIS – PROPOSED

METHOD

3.1. Breakdown into Symmetric and Asymmetric Jacobian Matrices

It is a known fact that the power system Jacobian matrix is a real quasi-symmetric matrix. If the ordinary Jacobian matrix were to be substituted by its symmetric part, then various distinctive properties of a real symmetric matrix can be utilized to further study the voltage instability problem.^[7] To facilitate this study, the existing Jacobian matrix is decomposed into two parts viz., symmetric and asymmetric. From the expression of Jacobian matrix equation, the symmetric (J_S) and asymmetric (J_{AS}) parts can be derived as,

$$J = \begin{bmatrix} \underline{J}^{P\theta} & \underline{J}^{PV} \\ \underline{J}^{Q\theta} & \underline{J}^{QV} \end{bmatrix} = J_S + J_{AS}$$

$$\text{Where, } J_S = \frac{1}{2}(J + J^T) = \begin{bmatrix} \underline{J}^{P\theta} + \underline{J}^{(P\theta)^T} & \underline{J}^{PV} + \underline{J}^{(Q\theta)^T} \\ \underline{J}^{Q\theta} + \underline{J}^{(PV)^T} & \underline{J}^{QV} + \underline{J}^{(QV)^T} \end{bmatrix}$$

$$J_{AS} = \frac{1}{2}(J - J^T) = \begin{bmatrix} \underline{J}^{P\theta} - \underline{J}^{(P\theta)^T} & \underline{J}^{PV} - \underline{J}^{(Q\theta)^T} \\ \underline{J}^{Q\theta} - \underline{J}^{(PV)^T} & \underline{J}^{QV} - \underline{J}^{(QV)^T} \end{bmatrix}$$

Thus the two parts of Jacobian, J_S and J_{AS} are used for further linear analysis treatment. Before jumping into the proposed method, for better understanding of these two matrices, few voltage stability indices are calculated based on this technical paper.^[6]

3.2. Formulation of Voltage Stability Indices from J_S and J_{AS}

Using the Singular Value Decomposition (SVD) technique, the singular value matrix can be obtained which is represented as the diagonal matrix of singular values. This singular value matrix is used to calculate the 2-norm and F-norm for calculating indices. The importance of singular values is that it can be used to assess the closeness of a matrix approaching a singular matrix. The SVD of Jacobian matrix can be expressed as:

$$J = W * \Sigma * V.$$

The singular value decomposition and the eigen decomposition are closely related.

- The left-singular vectors of J are eigen vectors of JJ^T .
- The right-singular vectors of J are eigenvectors of J^TJ .
- The non-zero-singular values of J (found on the diagonal entries of Σ) are the square roots of the non-zero eigen values of both J^TJ and JJ^T .

Our particular interest is to find the singular values found on the diagonal entries of the singular matrix with descending order in value. Analysis of norms and weighted singular values is considered as it relates to the error in order to analyze the singularity of the Jacobian.

Index 1: This is defined as the ratio of weighted sum of singular values of J_{AS} to the weighted sum of singular values of J_S .

Index 2: This is defined as the ratio of 2-norm of J_{AS} to the 2-norm of J_S .

Index 3: This is defined as the ratio of F-norm of J_{AS} to the F-norm of J_S .

Index 4: This is defined as the ratio of weighted sum of the difference of singular values J and J_S to the weighted sum of the difference of singular values J and J_{AS} .

Table 1 below shows the expression for all four indices.

Table 1. List of Indices and their expressions

Index	Expression	Description
Index 1	$\frac{M\sigma(J_{AS})}{M\sigma(J_S)}$	Weighted sum of singular values
Index 2	$\frac{Norm(J_{AS}, 2)}{Norm(J_S, 2)}$	2 norm
Index 3	$\frac{Norm(J_{AS}, 'fro')}{Norm(J_S, 'fro')}$	Frobenius Norm
Index 4	$\frac{M(\sigma(J) - \sigma(J_S))}{M(\sigma(J) - \sigma(J_{AS}))}$	Weighted sum of difference between singular values

a. Significance of Indices

The indices represent ratios of various norms, ratios of weighted singular values.

Norms represent the size of the vector and it is a tool to measure the error difference. In power flow analysis, the jacobian matrix becomes singular when the demand cannot meet

the required load and as a result when this happens, the matrix blows up and becomes singular and results in faults, short circuit, etc. Thus the indices presents a way to measure the error from the Jacobian form before it tends to become singular along a scale of loading factor.

b. Need for Indices

The main objective is to obtain J_{AS} which should tend to zero so that $J = J_S$. Hence that is the sufficient and necessary condition. As loading factor increases, the indices show that that J can be approximately replaced by J_S . In the index 1 it is sufficient for weighted sum of J_{AS} is zero. In the index 2 it is sufficient that 2-norm of J_{AS} is zero. In the index it is sufficient that F-norm of J_{AS} is zero. In the index four it is sufficient that the difference of weighted sum of J and J_S is zero, as this represents the error. Indices are a measure of when the jacobian becomes more symmetric as J_{AS} approaches zero when the load is increased.

c. Results from IEEE test systems

A MATLAB program was written to generate these indices by iteratively solving the load flow program at a constant load increment by keeping the same power factor. The program was run on three popular IEEE transmission level test systems and the figures 2,3, and 4 show the outputs on 14-bus, 30-bus and 118-bus systems respectively.

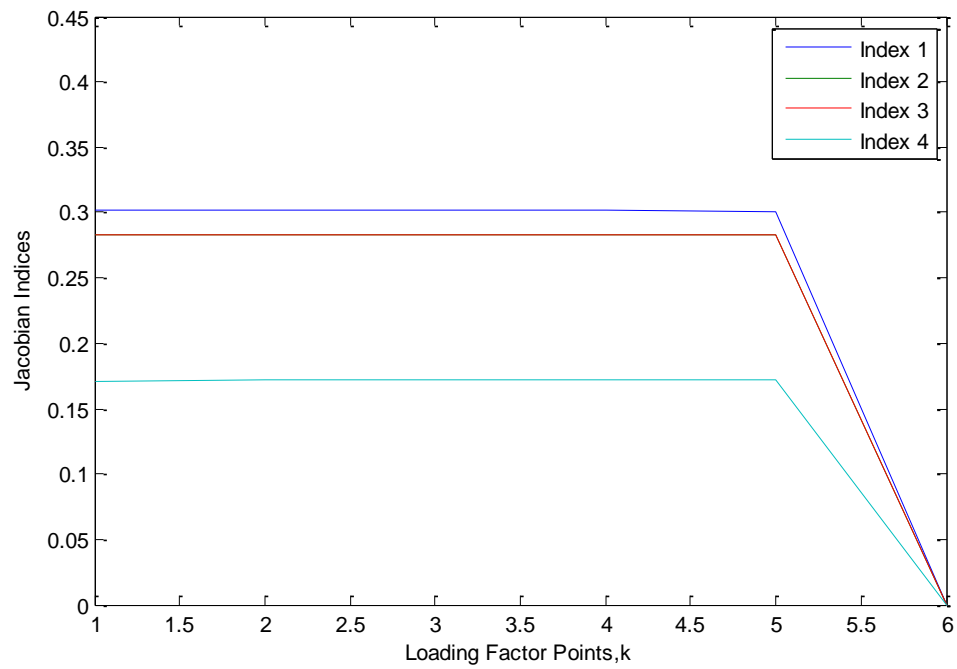


Figure 2. . Jacobian Indices on IEEE 14-bus

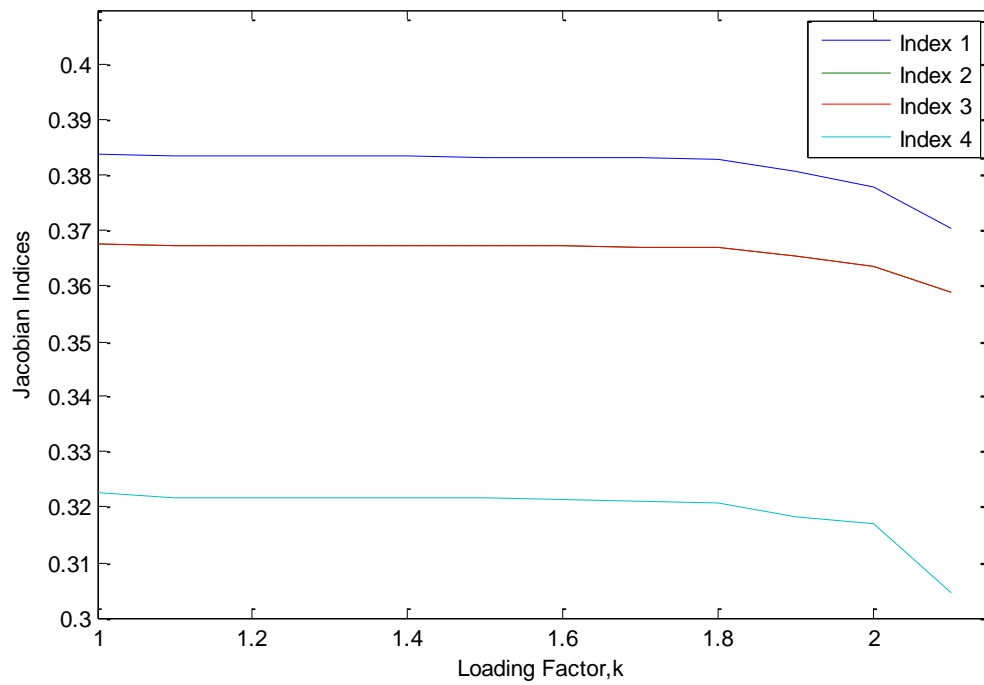


Figure 3. Jacobian Indices on IEEE 30-bus

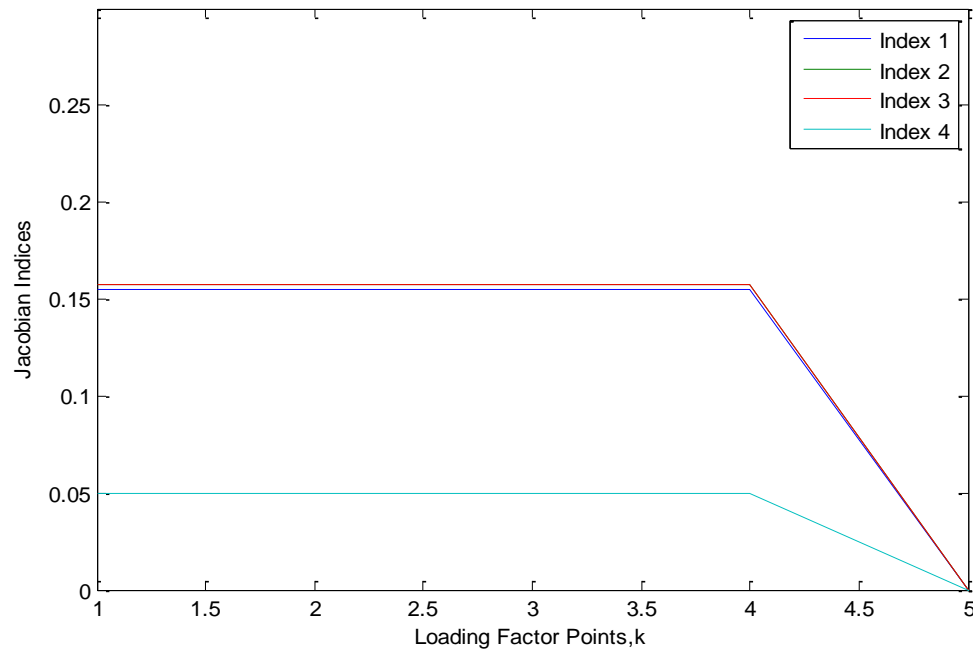


Figure 4. Jacobian Indices on IEEE 118-bus

3.3. GERSHGORIN CIRCLE THEOREMS

When dealing with eigenvalue decomposition of symmetric matrices, Gershgorin circle theorems emanates as a great tool for visual interpretation of the eigenvalues and the dominance of the diagonal elements. ^[8] There three important theorems concerning the eigenvalue decomposition of symmetric or strictly diagonally dominant matrices,

Theorem 1: Every eigenvalue of matrix A_{nn} satisfies:

$$|\lambda - A_{ii}| \leq \sum_{j \neq i} |A_{ij}|$$

In analyzing this theorem we see that every eigenvalue of the matrix A must be within a distance d of A_{ii} for some i. Since in general, eigenvalues are elements of C, we can visualize an eigenvalue as a point in the complex plane, where that point has to be within distance d of A_{ii} for some i.

Theorem 2: Every eigenvalue of a matrix A must lie in a Gershgorin disc corresponding to the columns of A .

From this theorem, we have the set of eigenvalues that are in both A and A^T . Because the rows of A^T correspond to the columns of A , the eigenvalues fall inside Gershgorin discs corresponding to the columns of A due to A^T obeying Theorem 1.

Theorem 3: A Subset G of the Gershgorin discs is called a disjoint group of discs if no disc in the group G intersects a disc which is not in G . If a disjoint group G contains (r) nonconcentric discs, then there are (r) eigenvalues.

Theorem 1 says that an eigenvalue always has to be within a disc, and due to the continuity of the eigenvalue's path there is no way that an eigenvalue can move from one isolated group to another isolated group without being found in a region outside of any disc. Being outside of a disc violates Theorem 1 and therefore, for every disjoint group G that has n discs in it must have n eigenvalues in it.

3.3.1. Application of Gershgorin circle theorem to IEEE test systems

By applying the above-mentioned theorems to the power system Jacobian matrix, Gerschgorin circles were plotted with the center as diagonal element J_{ii} and the radii as the sum of off-diagonal elements, J_{ij} . The eigenvalues from the symmetric and asymmetric parts of the same Jacobian matrix were embedded as a scatter plots in the circle to illustrate the theorems. Figure 6,7 and 8 show the Gershgorin circle plots for IEEE 14-bus, 30-bus and 118-bus system respectively. The green dots indicate eigenvalues of symmetric Jacobian matrix, J_S and the red dots indicate eigenvalues of asymmetric Jacobian matrix, J_{AS} .

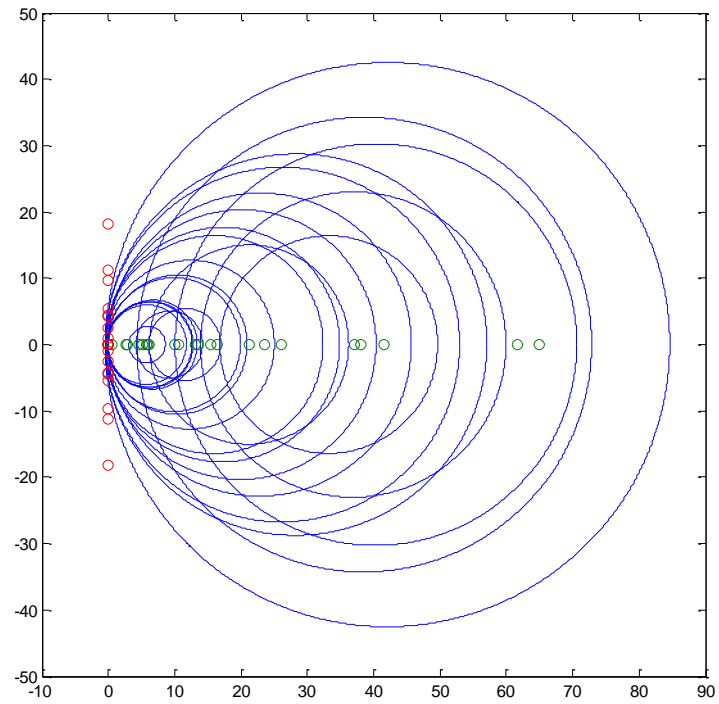


Figure 5. . Gershgorin circle plot for IEEE 14-bus system

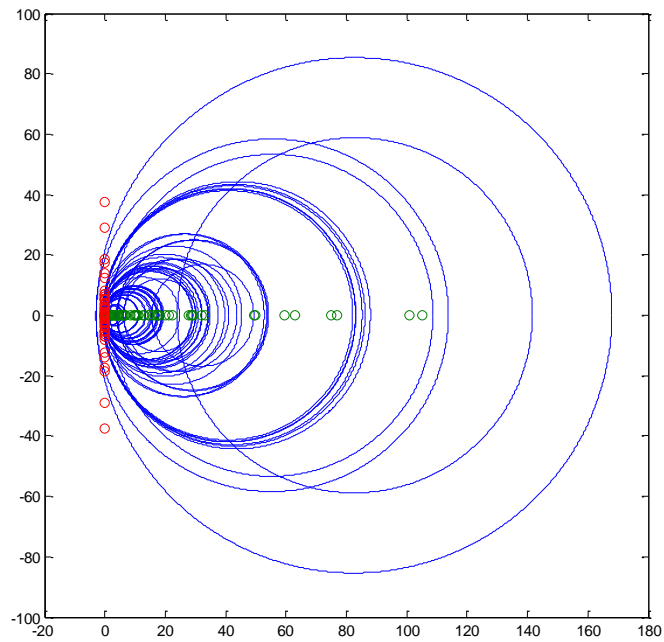


Figure 6. Gershgorin circle plot for IEEE 30-bus system

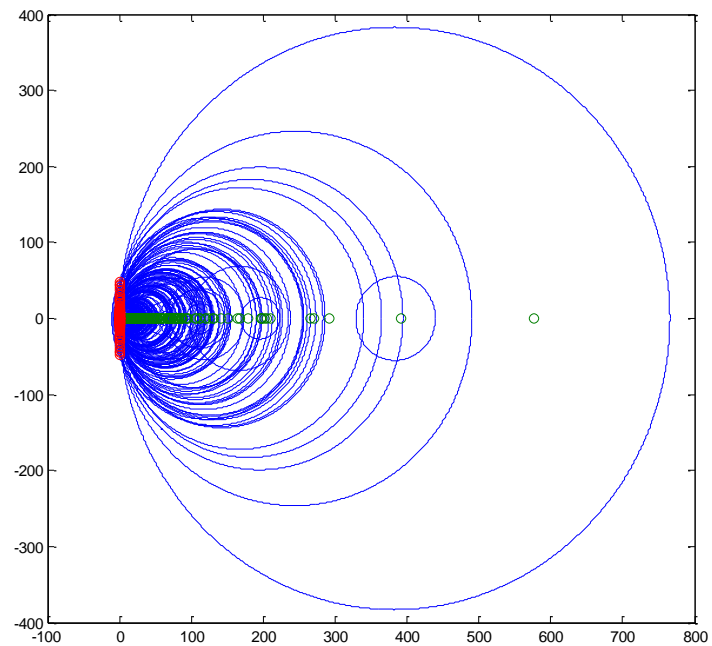


Figure 7. Gershgorin circle plot for IEEE 118-bus system

3.4. Modal Analysis of Symmetric Jacobian Matrix

As explained in the previous chapters, the significance of symmetric Jacobian matrix is now obvious. By using this approximate expression of ordinary power system Jacobian, the system is seen as a network of lossless transmission lines and hence the matrix is stronger and non-singular even in the nose-region of the PV curve. This facilitates robust calculation of eigenvalues and thereby better prediction of critical modes of the power system from the perspective of voltage stability. It is to be noted that modal analysis techniques are reliable only when the system is stressed and operated close to the nose-region. So, load-levels for each IEEE test systems viz. 14-bus,30-bus and 118-bus have been carefully chosen after several trials. This method has been rigorously tested in all these systems and comparative analysis of results have been shown in the coming chapters.

3.4.1. IEEE 14-bus test system

The IEEE 14 Bus Test Case represents a portion of the American Electric Power System (in the Midwestern US) as of February, 1962. It consists of 20 branches and the stable operating point at which the simulation was performed has a total system loading of 5.18 MW and reactive power injection of 1.626 MVAR. Figure 10 shows the mode shape of the system with the pink line denoting the symmetric Jacobian matrix while the blue line denoting the original Jacobian matrix. Figure 11 shows participation factors from both the proposed method (brown bar) and the conventional method (blue bar). It can be seen that both points to the bus 14 as the weakest bus in the sense that it is most

voltage sensitive to any reactive power injected into that bus. This is confirmed by the results from PV analysis in Figure 12 which shows bus 14 having the maximum voltage drop with increasing load.

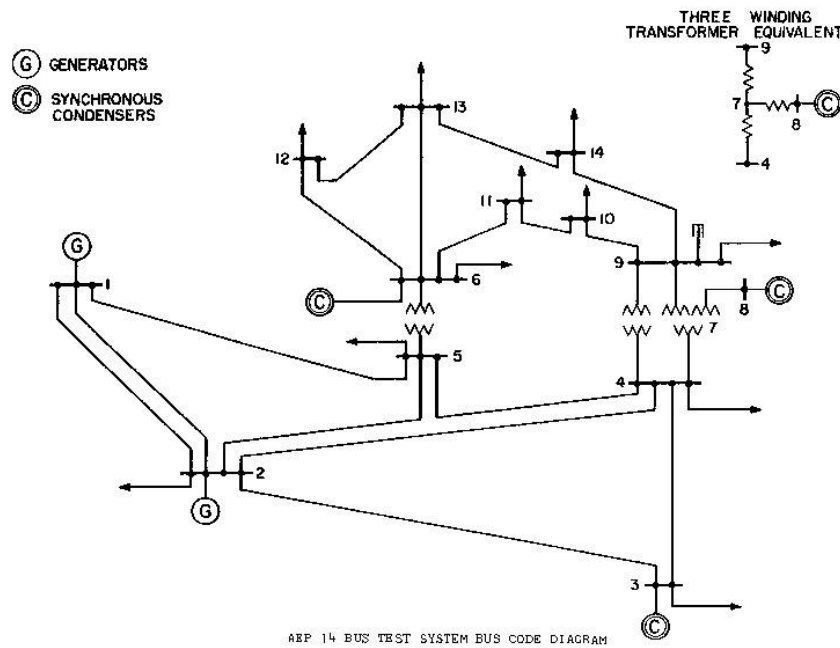


Figure 8. One line diagram - IEEE 14-bus test system

Table 2. Load and generation profile for IEEE 14-bus system

B.No	Type	Generation		Load	
		Real (MW)	Reactive (MW)	Real (MW)	Reactive (MW)
1	3	5.089735	27.2449	0	0
2	1	0.4	-13.9423	0.434	0.254
3	1	0.2	-7.64262	0.224	0.15
4	1	0	-39.1799	1.884	0.38
5	1	0	8.331325	0	0
6	2	0	0	0	0
7	2	0	0	0.59	0.332
8	2	0	0	0.152	0.032

9	2	0	0	0.956	0.078
10	2	0	0	0.18	0.116
11	2	0	0	0.07	0.036
12	2	0	0	0.122	0.032
13	2	0	0	0.27	0.116
14	2	0	0	0.298	0.1
Total		5.689735	-25.1886	5.18	1.626

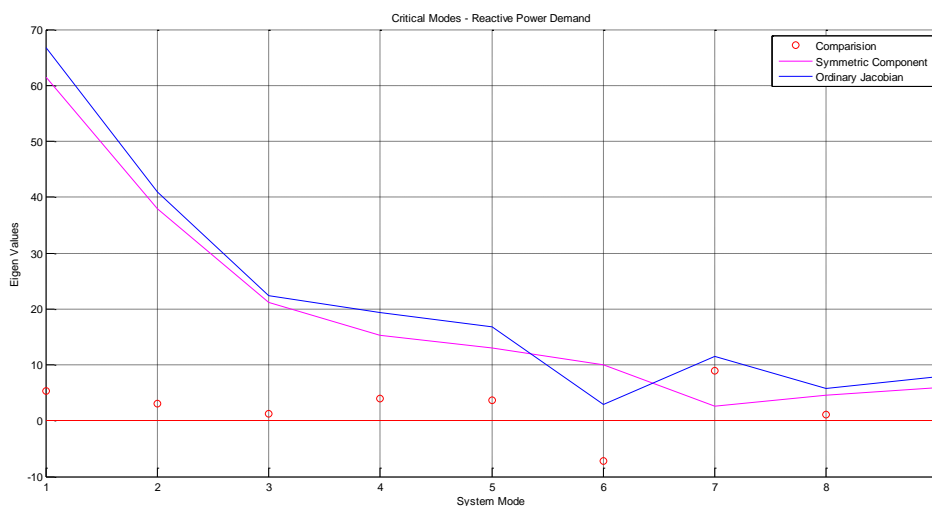


Figure 9. Mode Shape – IEEE 14-Bus system

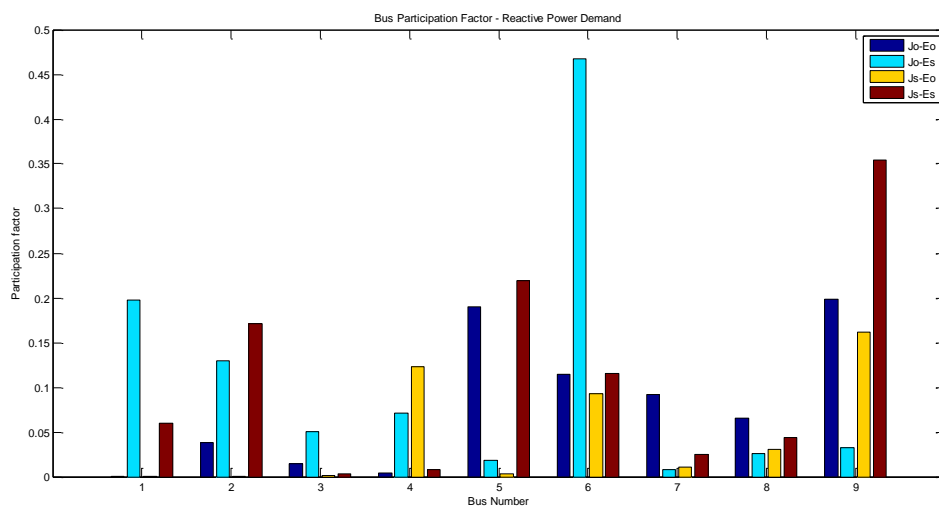


Figure 10. Participation factors – IEEE 14-Bus system

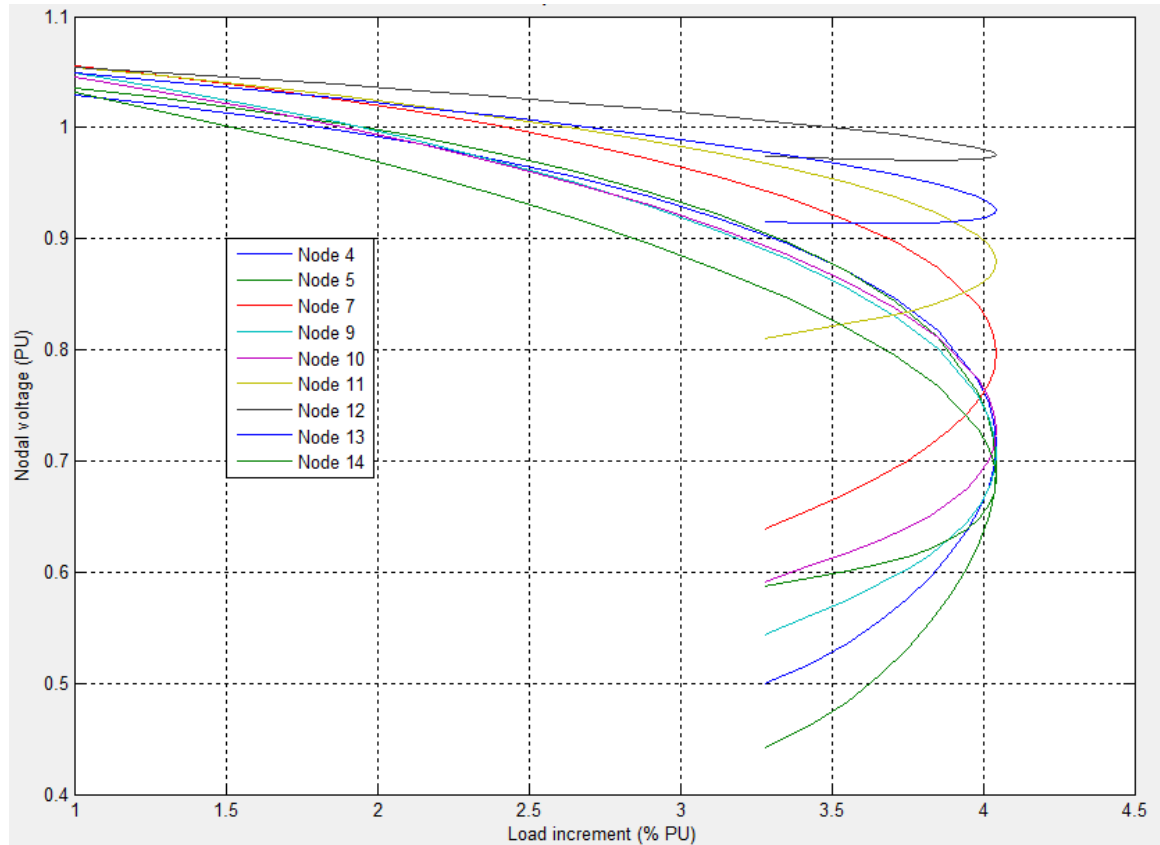


Figure 11. PV curves – IEEE 14-bus system

3.4.2. IEEE 30-bus test system

The IEEE 30 Bus Test Case represents a portion of the American Electric Power System (in the Midwestern US) as of December, 1961. It consists of 45 branches and the stable operating point at which the simulation was performed has a total system loading of 238 MW and reactive power injection of 160.8 MVAR. Figure 10 shows the mode shape of the system with the pink line denoting the symmetric Jacobian matrix while the blue line denoting the original Jacobian matrix. Figure 15 shows participation factors

from both the proposed method (brown bar) and the conventional method (blue bar). It can be seen that both points to the bus 26 as the weakest bus in the sense that it is most voltage sensitive to any reactive power injected into that bus. In this case, it more conspicuous that the magnitude of the participation factor from the proposed method is greatly larger than the conventional method. A scaled up version of the same plot is showed in Figure 16 to illustrate the participation factor from the conventional method. In this case, it can be established that proposed method suppresses the participation factors of non-participating buses (stronger buses) and magnifies the participation factors of weaker buses, thus, providing better prediction of weaker buses than the conventional method of modal analysis. This is confirmed by the results from PV analysis in Figure 17 which shows bus 26 having the maximum voltage drop with increasing load.

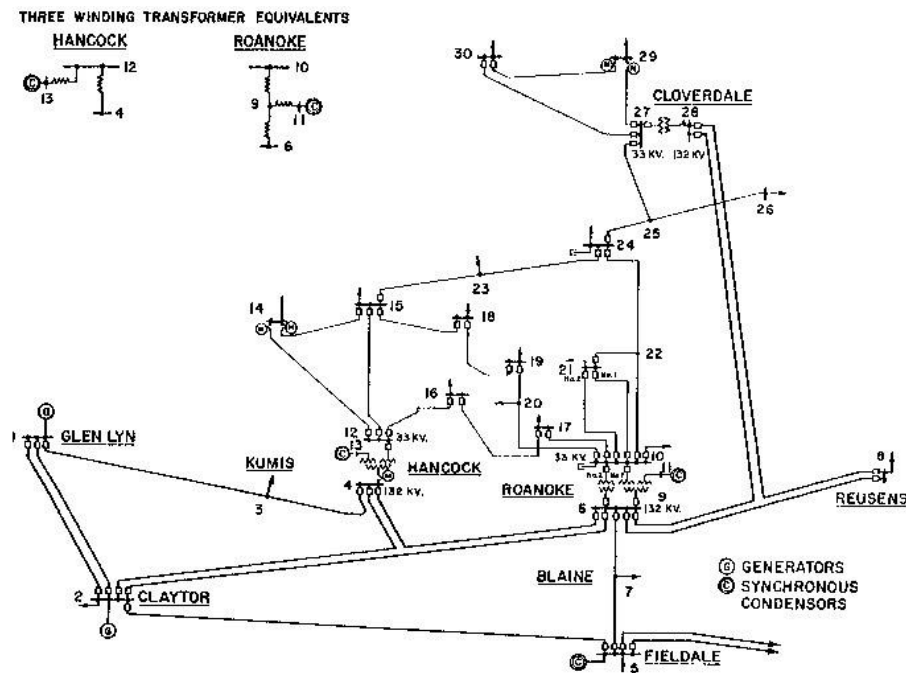


Figure 12. One line diagram - IEEE 30 Bus system

Table 3. Load and generation profile for IEEE 30-bus system

B.No	Type	Generation		Load	
		Real	Reactive	Real	Reactive
1	3	127.3345324	-22.73626374	0	0
2	1	60.97	70.94202899	32.55	19.05
3	2	0	0	3.6	1.8
4	2	0	0	11.4	2.4
5	2	0	0	0	0
6	2	0	0	0	0
7	2	0	0	34.2	16.35
8	2	0	0	45	45
9	2	0	0	0	0
10	2	0	0	8.7	3
11	2	0	0	0	0
12	2	0	0	16.8	11.25
13	1	37	17.22247706	0	0
14	2	0	0	9.3	2.4
15	2	0	0	12.3	3.75
16	2	0	0	5.25	2.7
17	2	0	0	13.5	8.7
18	2	0	0	4.8	1.35
19	2	0	0	14.25	5.1
20	2	0	0	3.3	1.05
21	2	0	0	26.25	16.8
22	1	21.58974359	62.0044843	0	0
23	1	19.2	17.29113924	4.8	2.4
24	2	0	0	13.05	10.05
25	2	0	0	0	0
26	2	0	0	5.25	3.45
27	1	26.91	18.75789474	0	0
28	2	0	0	0	0
29	2	0	0	3.6	1.35
30	2	0	0	15.9	2.85
Total		293.0045299	163.4816528	283.8	160.8

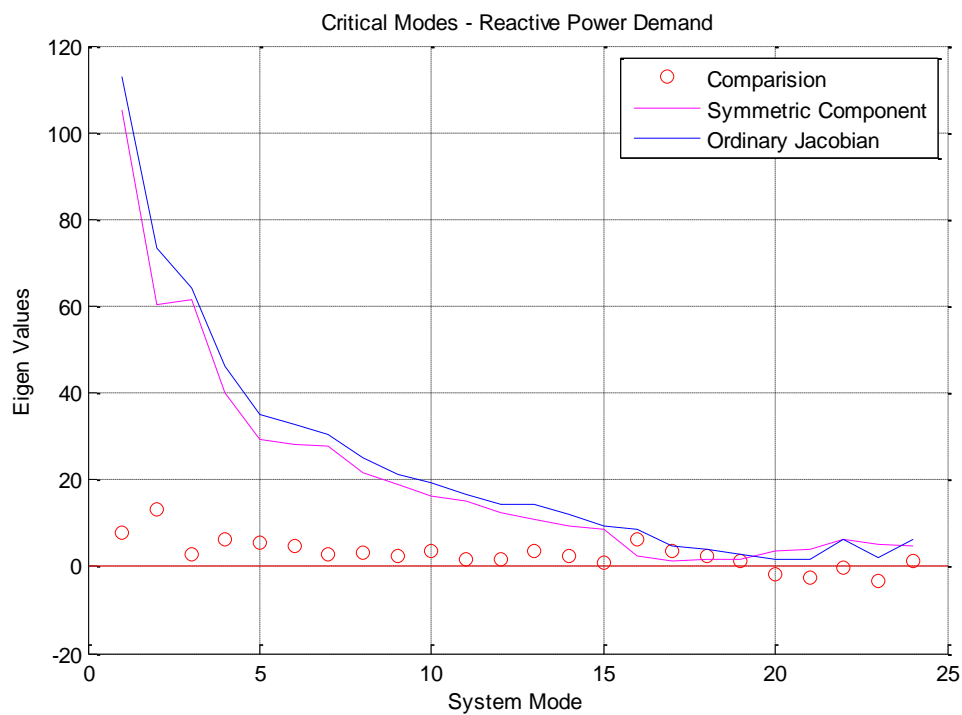


Figure 13. Mode Shape - IEEE 30 Bus system

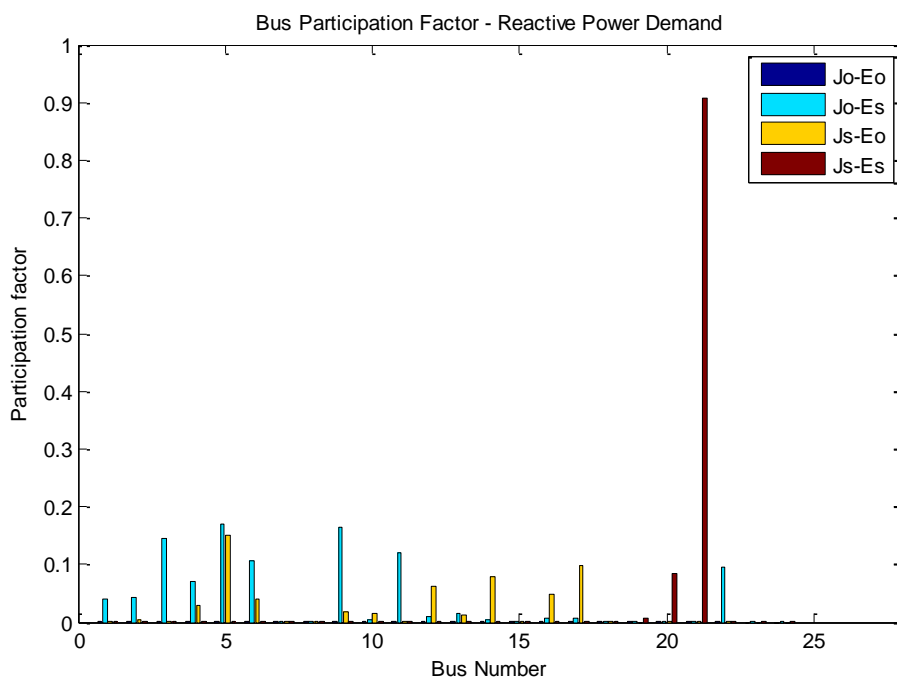


Figure 14. Bus Participation Factors - IEEE 30 Bus system

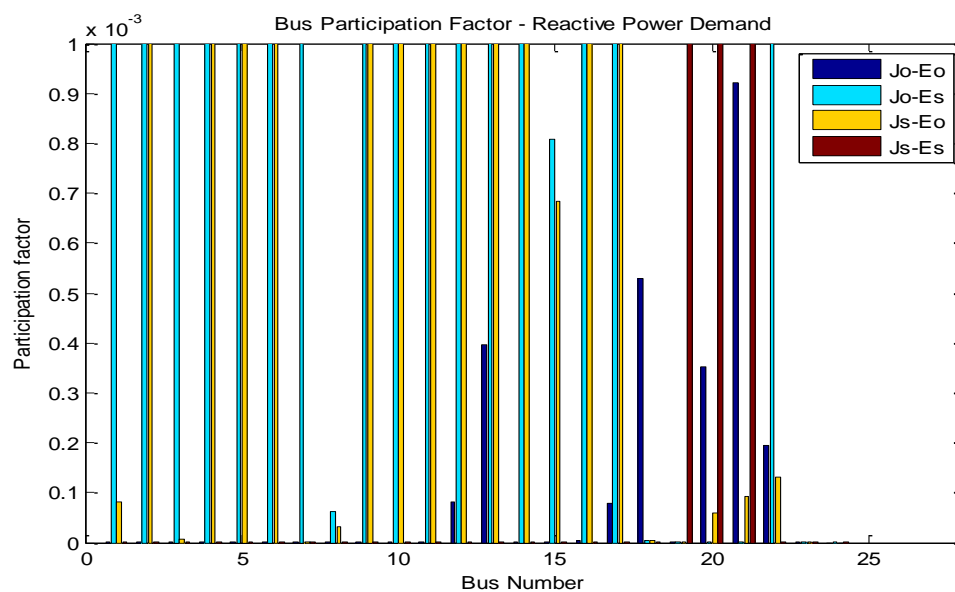


Figure 15. Bus Participation factors zoomed in by a factor of 1000 - IEEE 30 Bus system

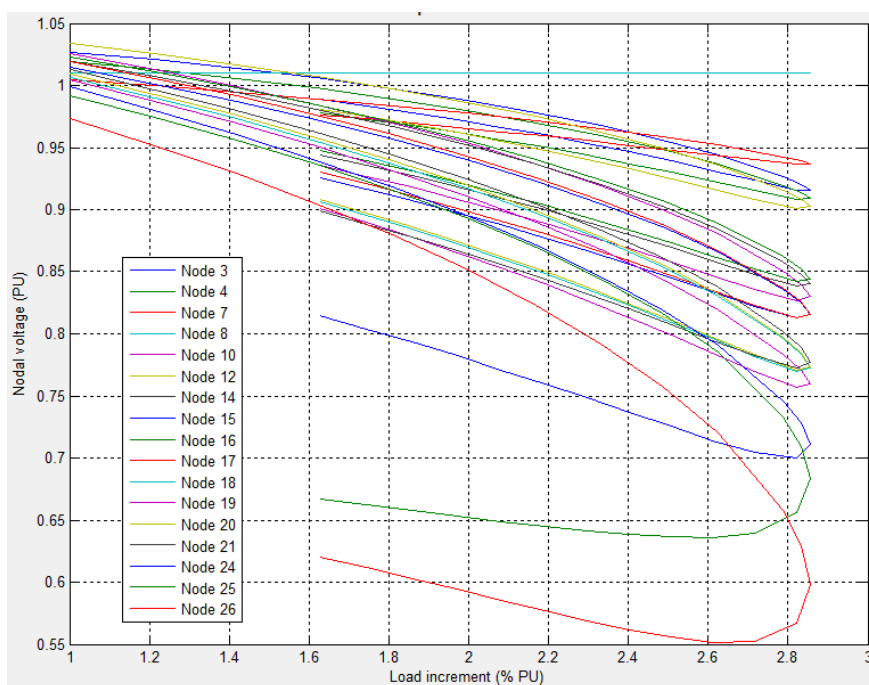


Figure 16. PV Curves - IEEE 30 Bus system

3.4.3. IEEE 118-bus test system

The 118-bus test system can be regarded as a realistic transmission level power network in terms of number of nodes and branches. It consists of 186 branches and represents a portion of the American Electric Power System (in the Midwestern US) as of December, 1962. The stable operating point at which the simulation was performed has a total system loading of 4369.26 MW and reactive power injection of 1481.14 MVAR. Figure 19 shows the mode shape of the system with the pink line denoting the symmetric Jacobian matrix while the blue line denoting the original Jacobian matrix. Figure 20 shows participation factors from both the proposed method (brown bar) and the conventional method (blue bar). It can be seen that proposed method points to the bus 21 as the weakest bus in the sense that it is most voltage sensitive to any reactive power injected into that bus, while the conventional method points to bus 71 as the weakest bus. This is confirmed by the results from PV analysis in Figure 21 which shows bus 21 having the maximum voltage drop with increasing load while bus 71 does not have a quick voltage drop to load growth. In addition to bus 21, the proposed method also shows considerable participation factors for bus 20 and 22 which indicates next weaker buses to bus 21. This is evident in the PV curves which also show higher voltage drops for the buses 20 and 22. Thus the proposed method performs well in the case of larger bus numbers as it is less prone to numerical errors in the vicinity of nose region unlike the conventional modal analysis method.

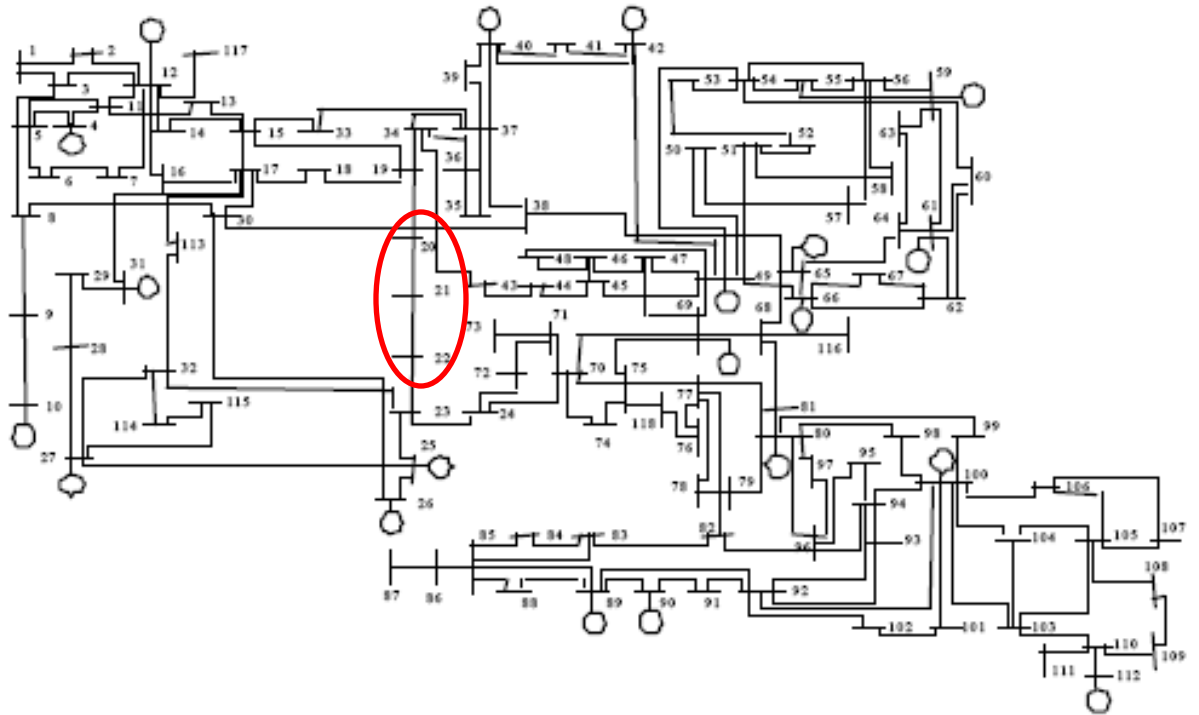


Figure 17. One-line diagram of IEEE 118-Bus system

Table 4. Load and generation profile for IEEE 118-bus system

B.No	Type	Generation		Load	
		Real	Reactive	Real	Reactive
1	3	819.975	-311.6666667	0	0
2	2	0	0	20.6	9.27027
3	2	0	0	40.16666667	10.3
4	1	0	-43.05	40.16666667	12.36
5	2	0	0	0	0
6	1	0	27.7173913	53.56	22.66
7	2	0	0	19.57142857	2.058824
8	1	0	-160.7179487	28.84	0
9	2	0	0	0	0
10	1	450	-216.8709677	0	0
11	2	0	0	72.1	23.68966
12	1	85	38.5	48.40909091	10.3
13	2	0	0	35.02	16.48
14	2	0	0	14.42105263	1.030303

B.No	Type	Generation		Load	
		Real	Reactive	Real	Reactive
15	1	0	11.9	92.7	30.9
16	2	0	0	25.75	10.3
17	2	0	0	11.33333333	3.090909
18	1	0	18.41176471	61.8	35.02
19	1	0	34.1875	46.35	25.75
20	2	0	0	18.53846154	3.090909
21	2	0	0	14.42105263	8.24
22	2	0	0	10.3	5.15
23	2	0	0	7.210526316	3.090909
24	1	0	-23.42857143	13.38888889	0
25	1	220	-166.4444444	0	0
26	1	314	20.72	0	0
27	1	0	31.3	73.13043478	13.38889
28	2	0	0	17.51020408	7.210526
29	2	0	0	24.72	4.12
30	2	0	0	0	0
31	1	7	31.69230769	44.28571429	27.80952
32	1	0	30.2	60.76923077	23.68966
33	2	0	0	23.69230769	9.27027
34	1	0	-96.85714286	60.76923077	26.78
35	2	0	0	33.99	9.27027
36	1	0	18.63333333	31.92857143	17.5102
37	2	0	0	0	0
38	2	0	0	0	0
39	2	0	0	27.80952381	11.33
40	1	0	46.76923077	67.98	23.68966
41	2	0	0	38.11111111	10.3
42	1	0	38.55	98.88	23.68966
43	2	0	0	18.53846154	7.210526
44	2	0	0	16.48	8.24
45	2	0	0	54.59090909	22.66
46	1	19	33.25806452	28.84	10.3
47	2	0	0	35.02	0
48	2	0	0	20.6	11.33
49	1	204	26.83333333	89.61111111	30.9
50	2	0	0	17.51020408	4.12
51	2	0	0	17.51020408	8.24
52	2	0	0	18.53846154	5.15
53	2	0	0	23.69230769	11.33

B.No	Type	Generation		Load	
		Real	Reactive	Real	Reactive
54	1	48	46.10526316	116.3888889	32.96
55	1	0	32.90909091	64.88888889	22.66
56	1	0	48.98412698	86.52	18.54
57	2	0	0	12.35714286	3.090909
58	2	0	0	12.35714286	3.090909
59	1	0	72.67391304	285.3076923	116.3889
60	2	0	0	80.34	3.090909
61	1	160	-44.8	0	0
62	1	0	32.14814815	79.30769231	14.42105
63	2	0	0	0	0
64	2	0	0	0	0
65	1	391	69.63636364	0	0
66	1	392	-231.7419355	40.16666667	18.54
67	2	0	0	28.84	7.210526
68	2	0	0	0	0
69	1	0	49.65	52.52941176	27.80952
70	1	0	24.125	67.98	20.6
71	2	0	0	0	0
72	1	0	-6.222222222	12.35714286	0
73	1	0	-2.15	6.181818182	0
74	1	0	60.97368421	70.04	27.80952
75	2	0	0	48.40909091	11.33
76	1	0	73.56818182	70.04	37.08
77	1	0	123.5238095	62.83333333	28.84
78	2	0	0	73.13043478	26.78
79	2	0	0	40.16666667	32.96
80	1	477	-154.1219512	133.9	26.78
81	2	0	0	0	0
82	2	0	0	55.62068966	27.80952
83	2	0	0	20.6	10.3
84	2	0	0	11.33333333	7.210526
85	1	0	36.34782609	24.72	15.45
86	2	0	0	21.62962963	10.3
87	1	4	-1.625	0	0
88	2	0	0	49.44	10.3
89	1	607	-114.6666667	0	0
90	1	0	78.17391304	167.8888889	43.25926
91	1	0	-2.193548387	10.3	0
92	1	0	40.6875	66.95	10.3

B.No	Type	Generation		Load	
		Real	Reactive	Real	Reactive
93	2	0	0	12.35714286	7.210526
94	2	0	0	30.9	16.48
95	2	0	0	43.25925926	31.92857
96	2	0	0	39.14285714	15.45
97	2	0	0	15.45	9.27027
98	2	0	0	35.02	8.24
99	1	0	2.785714286	43.25925926	0
100	1	252	-17.64285714	38.11111111	18.54
101	2	0	0	22.66	15.45
102	2	0	0	5.15	3.090909
103	1	40	9.714285714	23.69230769	16.48
104	1	0	29.66666667	39.14285714	25.75
105	1	0	40.07692308	31.92857143	26.78
106	2	0	0	44.28571429	16.48
107	1	0	23.46153846	51.5	12.36
108	2	0	0	2.058823529	1.030303
109	2	0	0	8.24	3.090909
110	1	0	25.97727273	40.16666667	30.9
111	1	36	-11.91666667	0	0
112	1	0	36.33707865	70.04	13.38889
113	1	0	-56.47826087	6.181818182	0
114	2	0	0	8.24	3.090909
115	2	0	0	22.66	7.210526
116	1	0	73.13333333	189.52	0
117	2	0	0	20.6	8.24
118	2	0	0	33.99	15.45
Total		4525.975291	-223.2599631	4369.26	1481.14

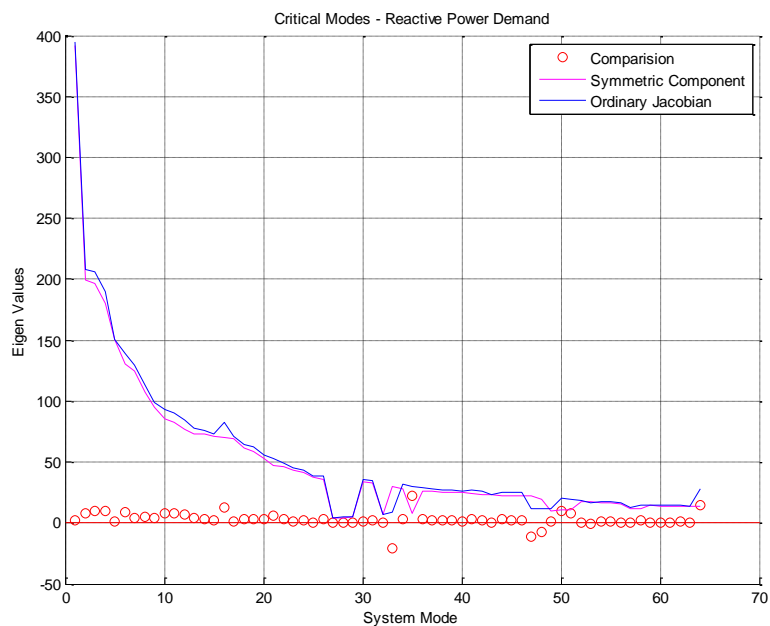


Figure 18. Mode Shape – IEEE 118 Bus system

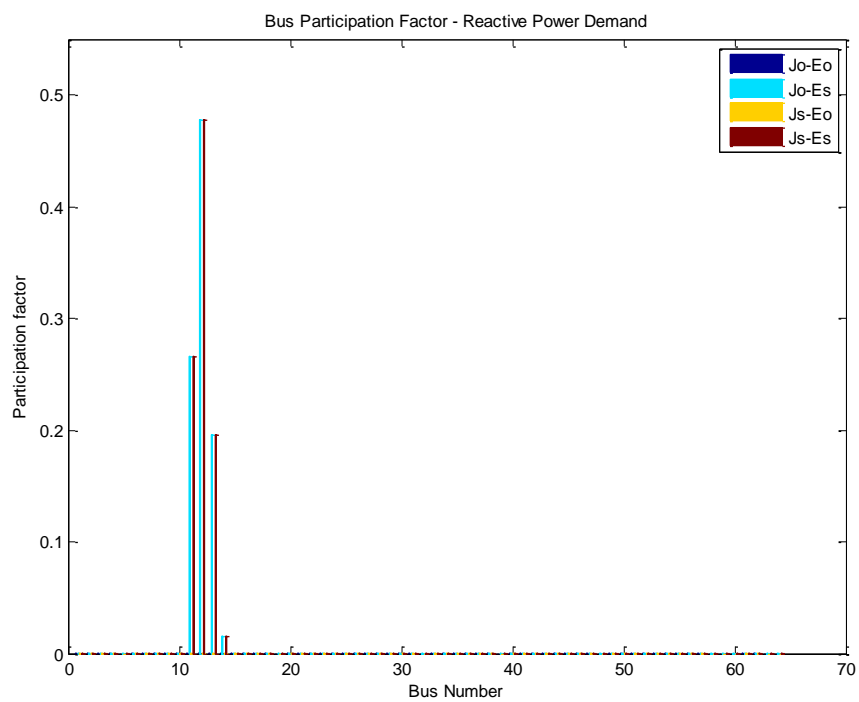


Figure 19. Bus Participation Factors – IEEE 118 Bus system

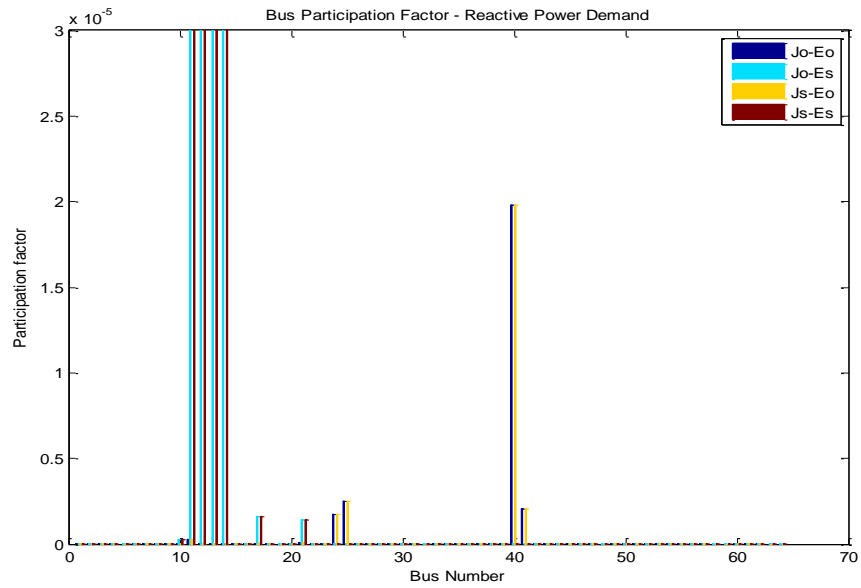


Figure 20. Bus Participation Factors scaled by a factor of 10000 – IEEE 118 Bus system

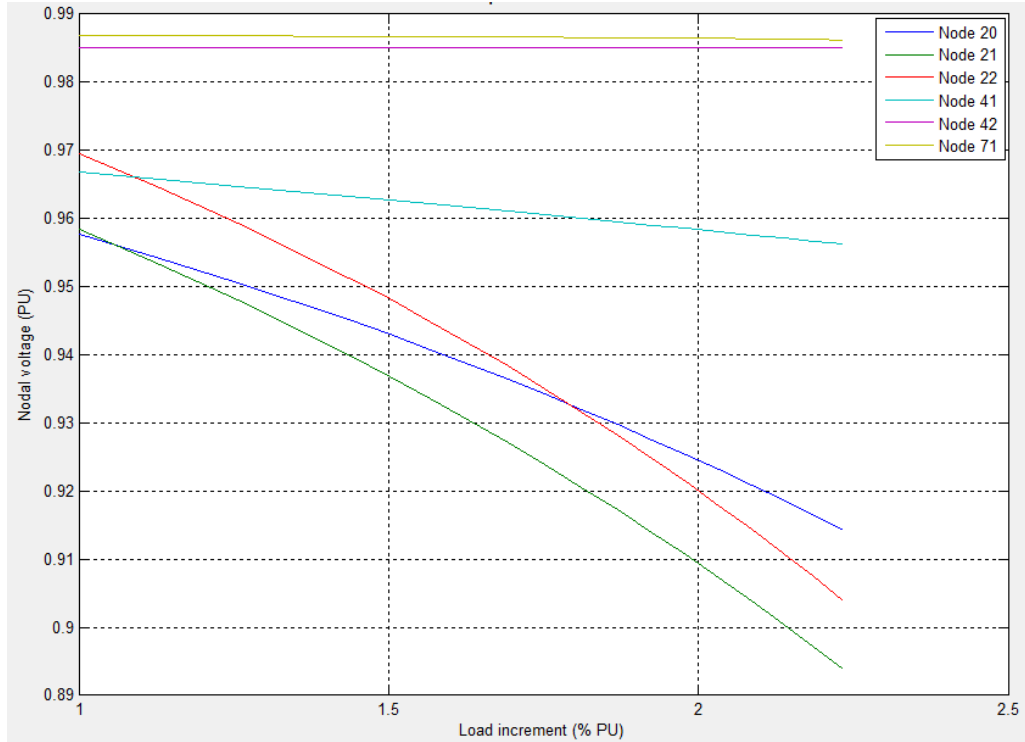


Figure 21. PV Curves of critical buses – IEEE 118 Bus system

4. FUTURE WORK

As discussed in the beginning of this thesis work, angle stability and voltage stability are closely associated when the system operates in the vicinity of nose region. So, it is important to consider the dynamics of the power system when studying about voltage instability. Also, in a realistic transmission network, there are thousands of nodes, branches and generators. It is necessary to breakdown the system into small areas and then conducts study on voltage stability. A method based on Principal Component Analysis has been proposed in these literatures^{[9][10]} which can be used to identify coherent generation groups and coherent buses from the time-stamped angular data and voltage data respectively. Three most significant principal components are chosen and their corresponding generator data or voltage data are plotted as coordinates in a three-dimensional plot. The coherent generator groups are then, visually formed by optimal rotation of the x, y and z-axes. After the buses are grouped together, modal analysis of symmetric Jacobian matrix can be performed on individual groups and weakest buses among each area can be effectively determined.

4.1. Simulation on the entire eastern interconnection

The simulation was performed on a 2013 Summer light load case consisting of 65440 buses, 61990 branches and 7947 generators representing the entire Eastern interconnection. All the generators, exciters, governors and loads have dynamic models present. A time-domain simulation was performed using Siemens PSS/E software following a 15 cycle fault at a BPS station. The time-stamped data of 21 generators were fed into a python program to perform the principal component analysis (PCA). Three most significant PCs were identified and plotted in three-dimensional plot. The plot was

rotated optimally for the best possible viewing of coherent groups. Table 5 and Table 6 show the correlation matrix of angle plots from 21 generators and three significant principal components respectively. Figure 23 shows the three dimensional plot illustrating the coherent groups formed by the coordinates generated from the principal component analysis. Figure 24,25 and 26 show the angular plots of generators belonging to each group confirming the results from principal component analysis. The large system can thus be divided into smaller groups and further modal analysis can be performed as per the proposed method.

Table 5. Correlation Matrix – From time-stamped angle data

Variables	21																				
Sample	285																				
	V1	V2	V3	V4	V5	V6	V7	V8	V9	V10	V11	V12	V13	V14	V15	V16	V17	V18	V19	V20	V21
Mean	47.6586	25.2374	24.8619	27.6793	24.6474	27.4412	21.5888	19.6962	22.4188	46.5191	28.2399	27.2569	10.0616	-1.1756	19.8958	19.0959	1.0202	68.7419	21.8039	2.3428	1.1446
St. Dev.	24.7674	17.5642	15.9844	14.3980	16.2842	13.0644	15.4291	16.6702	15.3420	14.2848	14.1985	17.1254	16.6475	15.6194	9.6614	19.6269	13.8692	25.4257	7.8705	8.9943	7.7166
Correlation	V1	V2	V3	V4	V5	V6	V7	V8	V9	V10	V11	V12	V13	V14	V15	V16	V17	V18	V19	V20	V21
V1	1.0000	0.9089	0.8625	0.8332	0.7830	0.8250	0.8031	0.8423	0.7999	0.7401	0.7621	0.5809	0.5745	0.5527	0.6201	0.3773	0.5939	0.9663	0.7903	0.8005	0.8011
V2	0.9089	1.0000	0.9847	0.9735	0.9478	0.9659	0.9548	0.9846	0.9580	0.9119	0.9295	0.7484	0.7366	0.7021	0.7688	0.4980	0.7433	0.8197	0.8799	0.9259	0.9109
V3	0.8625	0.9847	1.0000	0.9860	0.9766	0.9884	0.9813	0.9967	0.9835	0.9440	0.9633	0.7810	0.7747	0.7307	0.8056	0.5550	0.7876	0.7779	0.8930	0.9487	0.9309
V4	0.8332	0.9735	0.9860	1.0000	0.9857	0.9831	0.9813	0.9899	0.9921	0.9566	0.9831	0.8608	0.8380	0.8084	0.8757	0.6208	0.8517	0.7392	0.8528	0.9315	0.9136
V5	0.7830	0.9478	0.9766	0.9857	1.0000	0.9669	0.9647	0.9807	0.9821	0.9335	0.9710	0.8360	0.8149	0.7757	0.8452	0.6258	0.8246	0.6733	0.8146	0.9042	0.8828
V6	0.8250	0.9659	0.9884	0.9831	0.9669	1.0000	0.9971	0.9880	0.9873	0.9777	0.9833	0.8098	0.8057	0.7609	0.8473	0.6081	0.8326	0.7522	0.9260	0.9792	0.9658
V7	0.8031	0.9548	0.9813	0.9813	0.9647	0.9971	1.0000	0.9826	0.9890	0.9870	0.9897	0.8285	0.8298	0.7868	0.8669	0.6199	0.8557	0.7304	0.9137	0.9723	0.9586
V8	0.8423	0.9846	0.9967	0.9899	0.9807	0.9880	0.9826	1.0000	0.9891	0.9484	0.9684	0.7900	0.7811	0.7432	0.8165	0.5674	0.7919	0.7521	0.8820	0.9449	0.9266
V9	0.7999	0.9580	0.9835	0.9921	0.9821	0.9873	0.9890	0.9891	1.0000	0.9697	0.9895	0.8435	0.8388	0.8111	0.8795	0.6400	0.8542	0.7177	0.8612	0.9410	0.9237
V10	0.7401	0.9119	0.9440	0.9566	0.9335	0.9777	0.9870	0.9484	0.9697	1.0000	0.9836	0.8509	0.8513	0.8122	0.8901	0.6587	0.8839	0.6696	0.9001	0.9630	0.9571
V11	0.7621	0.9295	0.9633	0.9831	0.9710	0.9833	0.9897	0.9684	0.9895	0.9836	1.0000	0.8872	0.8664	0.8339	0.9138	0.6765	0.8964	0.6861	0.8644	0.9450	0.9305
V12	0.5809	0.7484	0.7810	0.8608	0.8360	0.8098	0.8285	0.7900	0.8435	0.8509	0.8872	1.0000	0.9259	0.9215	0.9495	0.6760	0.9467	0.4970	0.6313	0.7456	0.7302
V13	0.5745	0.7366	0.7747	0.8380	0.8149	0.8057	0.8298	0.7811	0.8388	0.8513	0.8664	0.9259	1.0000	0.9703	0.9354	0.6617	0.9743	0.4968	0.6551	0.7552	0.7329
V14	0.5527	0.7021	0.7307	0.8084	0.7757	0.7609	0.7868	0.7432	0.8111	0.8122	0.8339	0.9215	0.9703	1.0000	0.9359	0.6747	0.9482	0.4870	0.5881	0.7023	0.6832
V15	0.6201	0.7688	0.8056	0.8757	0.8452	0.8473	0.8669	0.8165	0.8795	0.8901	0.9138	0.9495	0.9354	0.9359	1.0000	0.7670	0.9788	0.5688	0.6908	0.8016	0.7901
V16	0.3773	0.4980	0.5550	0.6208	0.6258	0.6081	0.6199	0.5674	0.6400	0.6587	0.6765	0.6760	0.6617	0.6747	0.7670	1.0000	0.7272	0.3190	0.4410	0.5741	0.5815
V17	0.5939	0.7433	0.7876	0.8517	0.8246	0.8326	0.8557	0.7919	0.8542	0.8839	0.8964	0.9467	0.9743	0.9482	0.9788	0.7272	1.0000	0.5359	0.6981	0.7954	0.7817
V18	0.9663	0.8197	0.7779	0.7392	0.6733	0.7522	0.7304	0.7521	0.7177	0.6696	0.6861	0.4970	0.4968	0.4870	0.5688	0.3190	0.5359	1.0000	0.7705	0.7566	0.7652
V19	0.7903	0.8799	0.8930	0.8528	0.8146	0.9260	0.9137	0.8820	0.8612	0.9001	0.8644	0.6313	0.6551	0.5881	0.6908	0.4410	0.6981	0.7705	1.0000	0.9783	0.9773
V20	0.8005	0.9259	0.9487	0.9315	0.9042	0.9792	0.9723	0.9449	0.9410	0.9630	0.9450	0.7456	0.7552	0.7023	0.8016	0.5741	0.7954	0.7566	0.9783	1.0000	0.9949
V21	0.8011	0.9109	0.9309	0.9136	0.8828	0.9658	0.9586	0.9266	0.9237	0.9571	0.9305	0.7302	0.7329	0.6832	0.7901	0.5815	0.7817	0.7652	0.9773	0.9949	1.0000
	1	2	3	4	5	6	7	8	9	10	11	12	13	14	15	16	17	18	19	20	21
Eigenvalues	17.7282	1.7168	0.5329	0.4384	0.3369	0.0956	0.0454	0.0384	0.0227	0.0200	0.0101	0.0061	0.0034	0.0020	0.0012	0.0007	0.0005	0.0003	0.0001	0.0000	0.0001

Table 6. Most Significant Principal Components

PCA	PCA1	PCA2	PCA3
V1	0.1953	-0.3270	0.4494
V2	0.2262	-0.1874	0.0709
V3	0.2311	-0.1334	-0.0434
V4	0.2346	-0.0315	0.0125
V5	0.2290	-0.0167	-0.0862
V6	0.2347	-0.0852	-0.1325
V7	0.2352	-0.0488	-0.1310
V8	0.2314	-0.1116	-0.0713
V9	0.2346	-0.0189	-0.0718
V10	0.2326	0.0202	-0.1955
V11	0.2354	0.0381	-0.1049
V12	0.2076	0.2986	0.1742
V13	0.2073	0.3082	0.2023
V14	0.1997	0.3430	0.2964
V15	0.2161	0.2781	0.1231
V16	0.1572	0.3488	-0.2572
V17	0.2131	0.2986	0.1321
V18	0.1785	-0.3614	0.5161
V19	0.2109	-0.2374	-0.2431
V20	0.2274	-0.1324	-0.2275
V21	0.2246	-0.1418	-0.2329

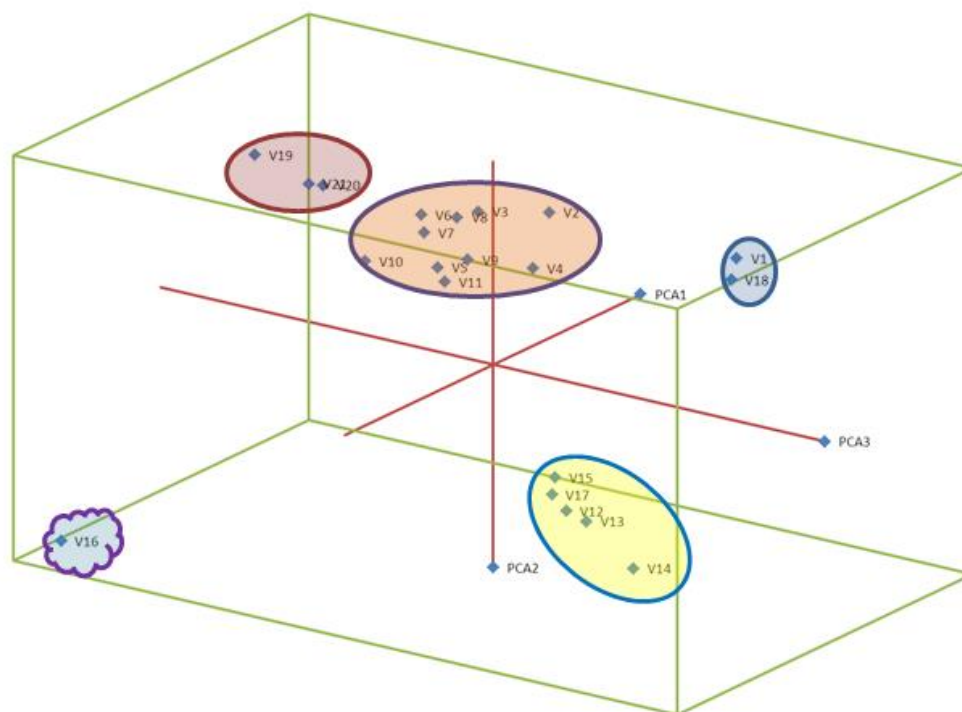


Figure 22. Three-dimensional plot with coherent groups forming distinct areas

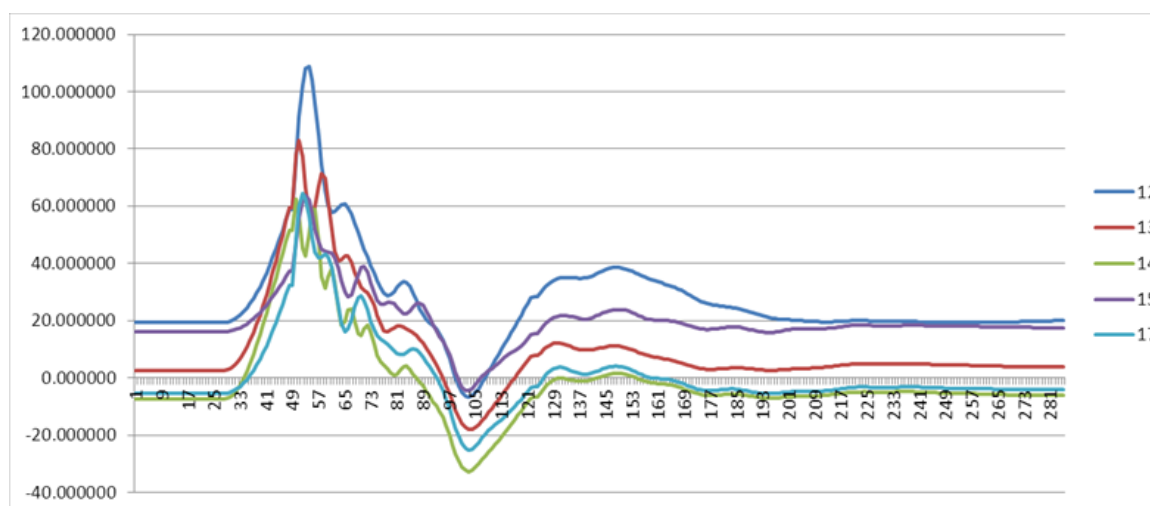


Figure 23. Angular Plot of Group 1

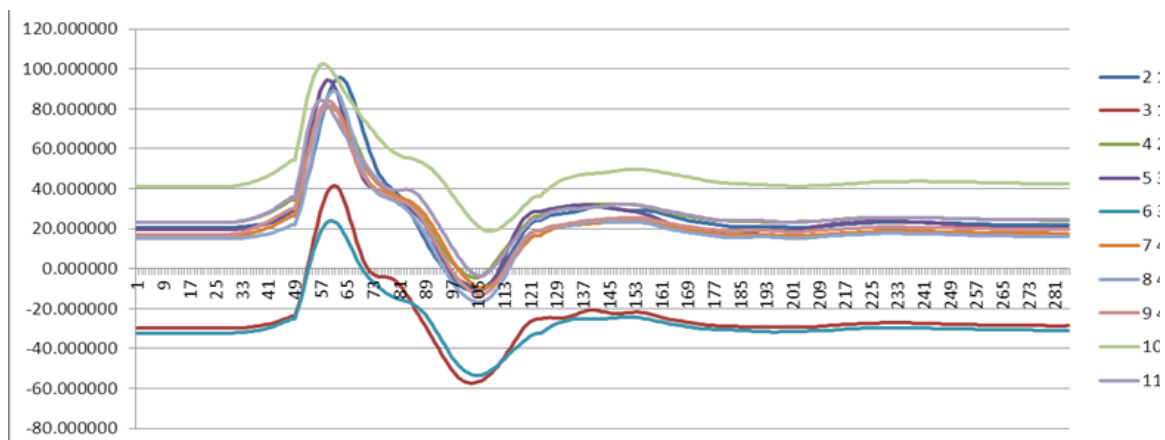


Figure 24. Angular Plot of Group 2

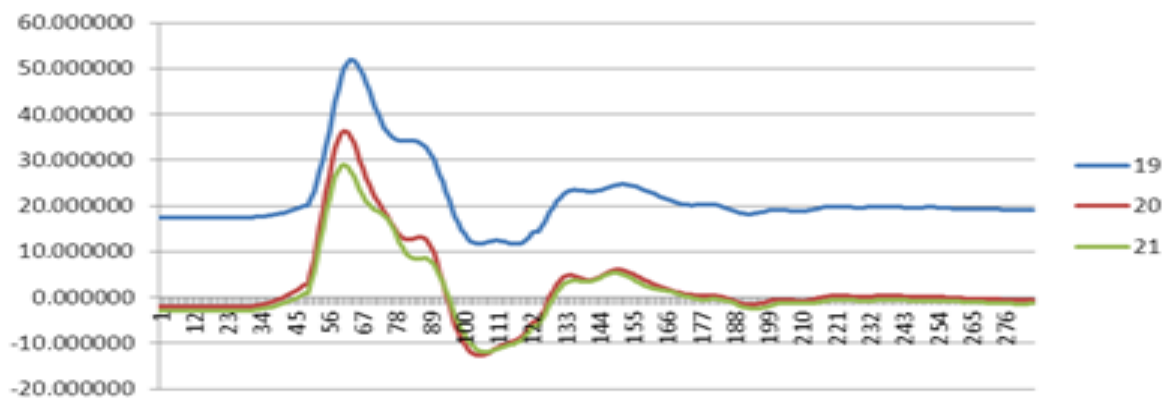


Figure 25. Angular Plot of Group 3

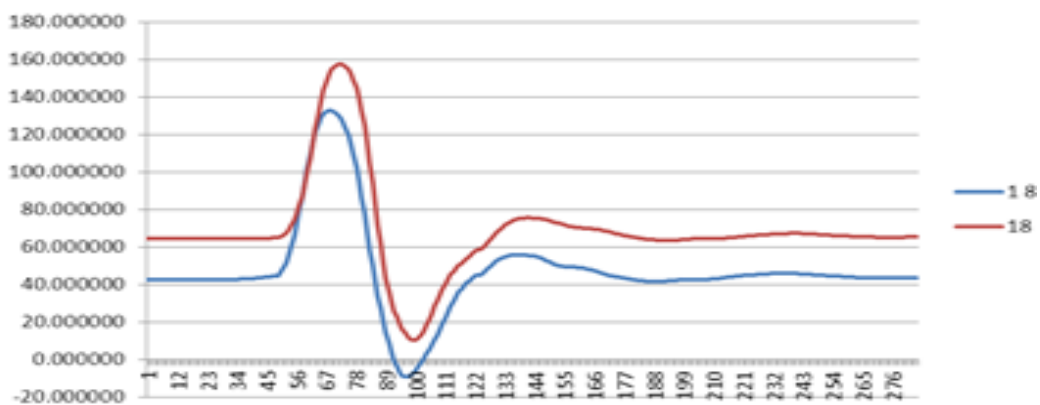


Figure 26. Angular Plot of Group 4

5. CONCLUSION

The main aim of this thesis work was to investigate the power system operating near the voltage collapse region and to provide a resilient method based on linear algebraic tool that is devoid of numerical insecurities. The proposed modal analysis of Symmetric Jacobian matrix has thus been proven efficient over the convention modal analysis in large power transmission network data. As shown by the results from simulations of three popular and well-accepted benchmark test systems namely, IEEE 14-bus, 30-bus and 118-bus system, it is clear that the proposed method is successful in identifying weaker with better accuracy than the conventional method.

Although, it is able to find the weakest nodes in the power grid, this method should be used in conjunction with PV curves for further details and mechanisms of voltage collapse of a particular node. This method can be used to narrow down the search for weaker buses but cannot be used as the only tool for voltage stability analysis. Future work indicates promising results for partitioning a larger power system into smaller groups and thus by combining both dynamic and steady-state analysis, more robust results are obtained. Further research in this method should also involve testing of real-life present-day power network to identify challenges that needs to be addressed.

6. REFERENCES

- [1] Atputharajah, A.; Saha, T.K., "Power system blackouts - literature review," *Industrial and Information Systems (ICIIS), 2009 International Conference on* , vol., no., pp.460,465, 28-31 Dec. 2009
- [2] Per-Anders Löf., "Study of Long Term Voltage Stability in Electric Power Systems", *Doctoral Thesis (KTH University)*, 1991
- [3] Lee, B.H.; Lee, K.Y., "A study on voltage collapse mechanism in electric power systems," *Power Systems, IEEE Transactions on* , vol.6, no.3, pp.966,974, Aug 1991
- [4] Ricardo Vargas, M.A Arjona and Manuel Carrillo (2011). PV Curves for Steady-State Security Assessment with MATLAB, MATLAB for Engineers - Applications in Control, Electrical Engineering, IT and Robotics, Dr. Karel Perutka (Ed.), ISBN: 978-953-307-914-1, InTech
- [5] Lof, P.-A.; Andersson, G.; Hill, D.J., "Voltage stability indices for stressed power systems," *Power Systems, IEEE Transactions on* , vol.8, no.1, pp.326,335, Feb 1993
- [6] Gao, B.; Morison, G. K.; Kundur, P., "Voltage stability evaluation using modal analysis," *Power Systems, IEEE Transactions on* , vol.7, no.4, pp.1529,1542, Nov 1992
- [7] Zhiyou Xu; Qingquan Jia; Liu Li, "The approximate expression of power flow jacobian matrix and analysis," *Sustainable Power Generation and Supply, 2009. SUPERGEN '09. International Conference on* , vol., no., pp.1,4, 6-7 April 2009
- [8] Curran, Paul F., "On a variation of the Gershgorin circle theorem with applications to stability theory," *Signals and Systems Conference (ISSC 2009), IET Irish* , vol., no., pp.1,5, 10-11 June 2009
- [9] Anaparthi, K.K.; Chaudhuri, B.; Thornhill, N.F.; Pal, B.C., "Coherency Identification in Power Systems Through Principal Component Analysis," *Power Systems, IEEE Transactions on* , vol.20, no.3, pp.1658,1660, Aug. 2005
- [10] Ariff, M.A.M.; Pal, B.C., "Coherency Identification in Interconnected Power System—An Independent Component Analysis Approach," *Power Systems, IEEE Transactions on* , vol.28, no.2, pp.1747,1755, May 2013

APPENDICES: MATLAB PROGRAMS

Appendix A. Admittance matrix calculation:

```

function Ymat = ybus(num,line)
%ieee_bus=5;
ieee_line=line;
switch num
    case 5
        data='IEEE5.xlsx';
    case 14
        data='IEEE14.xlsx';
    case 30
        data='IEEE30.xlsx';
    case 118
        data='IEEE118.xlsx';
end
sb=xlsread(data,1,sprintf('A2:A%d',(1+ieee_line)));
eb=xlsread(data,1,sprintf('B2:B%d',(1+ieee_line)));
R=xlsread(data,1,sprintf('C2:C%d',(1+ieee_line)));
X=xlsread(data,1,sprintf('D2:D%d',(1+ieee_line)));
Ys=xlsread(data,1,sprintf('E2:E%d',(1+ieee_line)));
Tap=xlsread(data,1,sprintf('F2:F%d',(1+ieee_line)));
Z=R+1i*X;
Y=1./Z;
Ys=1i*Ys;

n_bus=max(max(sb),max(eb));
n_branch=length(sb);
Ymat=zeros(n_bus,n_bus);

for k = 1:n_branch
    Ymat(sb(k),eb(k)) = Ymat(sb(k),eb(k)) - Y(k)/Tap(k);
    Ymat(eb(k),sb(k)) = Ymat(sb(k),eb(k));
end

for m = 1:n_bus
    for n = 1:n_branch
        if sb(n) == m
            Ymat(m,m) = Ymat(m,m) + Y(n)/(Tap(n)^2) + Ys(n);
        elseif eb(n) == m
            Ymat(m,m) = Ymat(m,m) + Y(n) + Ys(n);
        end
    end
end
end

```

Appendix B. Custom Load flow program – Individual Bus Investigation

```

function[] = custom_load_flow(busno,line,base,lnb)
ieee_bus=busno;
Ymatrix=ybus(ieee_bus,line);
switch busno
    case 5
        data='IEEE5.xlsx';
    case 14
        data='IEEE14.xlsx';
    case 30
        data='IEEE30.xlsx';
    case 118
        data='IEEE118.xlsx';
end
base_MVA=base;
Type=xlsread(data,2,sprintf('B3:B%d',(2+ieee_bus)));
Pg=xlsread(data,2,sprintf('C3:C%d',(2+ieee_bus)));
Qg=xlsread(data,2,sprintf('D3:D%d',(2+ieee_bus)));
Pl=xlsread(data,2,sprintf('E3:E%d',(2+ieee_bus)));
Ql=xlsread(data,2,sprintf('F3:F%d',(2+ieee_bus)));
Vol=xlsread(data,2,sprintf('G3:G%d',(2+ieee_bus)));
Qmin=xlsread(data,2,sprintf('H3:H%d',(2+ieee_bus)));
Qmax=xlsread(data,2,sprintf('I3:I%d',(2+ieee_bus)));
Delta=xlsread(data,2,sprintf('J3:J%d',(2+ieee_bus)));
Pg=Pg/base_MVA;
Qg=Qg/base_MVA;
Pl=Pl/base_MVA;
Ql=Ql/base_MVA;
lf=0.25;
q=1;
%l=1;
lf_max = 20;
while(lf<=lf_max)
    Pl(lnb,1)=lf*Pl(lnb,1);
    %Ql=1*Ql;
Qmin=Qmin/base_MVA;
Qmax=Qmax/base_MVA;
P=Pg-Pl;
Q=Qg-Ql;
Pspec=P;
Qspec=Q;
G=real(Ymatrix);
B=imag(Ymatrix);
PV=find(Type==1 | Type==3); %PV
PQ=find(Type==2); %PQ
n_PV=length(PV);
n_PQ=length(PQ);
n_bus=length(Vol);
Tolerance=10000000;
Iteration=1;
tic;
while(Tolerance>0.0001)
    P = zeros(n_bus,1);
    Q = zeros(n_bus,1);

```

```

for i = 1:n_bus
    for k = 1:n_bus
        P(i) = P(i) + Vol(i)* Vol(k)*(G(i,k)*cos(Delta(i)-Delta(k))
+ B(i,k)*sin(Delta(i)-Delta(k)));
        Q(i) = Q(i) + Vol(i)* Vol(k)*(G(i,k)*sin(Delta(i)-Delta(k))
- B(i,k)*cos(Delta(i)-Delta(k)));
    end
end

dPa = Pspec-P;
dQa = Qspec-Q;
k = 1;
dQ = zeros(n_PQ,1);
for i = 1:n_bus
    if Type(i) == 2
        dQ(k,1) = dQa(i);
        k = k+1;
    end
end
dP = dPa(2:n_bus);
Del_PQ = [dP; dQ];

J1 = zeros(n_bus-1,n_bus-1);
for i = 1:(n_bus-1)
    k = i+1;
    for j = 1:(n_bus-1)
        m = j+1;
        if m == k
            for m = 1:n_bus
                J1(i,j) = J1(i,j) + Vol(k)* Vol(m)*(-
G(k,m)*sin(Delta(k)-Delta(m)) + B(k,m)*cos(Delta(k)-Delta(m)));
            end
            J1(i,j) = J1(i,j) - Vol(k)^2*B(k,k);
        else
            J1(i,j) = Vol(k)* Vol(m)*(G(k,m)*sin(Delta(k)-Delta(m))
- B(k,m)*cos(Delta(k)-Delta(m)));
        end
    end
end
J2 = zeros(n_bus-1,n_PQ);
for i = 1:(n_bus-1)
    k = i+1;
    for j = 1:n_PQ
        m = PQ(j);
        if m == k
            for m = 1:n_bus
                J2(i,j) = J2(i,j) + Vol(m)*(G(k,m)*cos(Delta(k)-
Delta(m)) + B(k,m)*sin(Delta(k)-Delta(m)));
            end
            J2(i,j) = J2(i,j) + Vol(k)*G(k,k);
        else
            J2(i,j) = Vol(k)*(G(k,m)*cos(Delta(k)-Delta(m)) +
B(k,m)*sin(Delta(k)-Delta(m)));
        end
    end
end

```

```

end
J3 = zeros(n_PQ,n_bus-1);
for i = 1:(n_PQ)
    k = PQ(i);
    for j = 1:(n_bus-1)
        m = j+1;
        if m == k
            for m = 1:n_bus
                J3(i,j) = J3(i,j) + Vol(k)*
Vol(m)*(G(k,m)*cos(Delta(k)-Delta(m)) + B(k,m)*sin(Delta(k)-Delta(m)));
            end
            J3(i,j) = J3(i,j) - Vol(k)^2*G(k,k);
        else
            J3(i,j) = Vol(k)* Vol(m)*(-G(k,m)*cos(Delta(k)-
Delta(m)) - B(k,m)*sin(Delta(k)-Delta(m)));
        end
    end
end
end
J4 = zeros(n_PQ,n_PQ);
for i = 1:(n_PQ)
    k = PQ(i);
    for j = 1:n_PQ
        m = PQ(j);
        if m == k
            for m = 1:n_bus
                J4(i,j) = J4(i,j) + Vol(m)*(G(k,m)*sin(Delta(k)-
Delta(m)) - B(k,m)*cos(Delta(k)-Delta(m)));
            end
            J4(i,j) = J4(i,j) - Vol(k)*B(k,k);
        else
            J4(i,j) = Vol(k)*(G(k,m)*sin(Delta(k)-Delta(m)) -
B(k,m)*cos(Delta(k)-Delta(m)));
        end
    end
end
end
J=[J1 J2; J3 J4];
Del_x=J\Del_PQ;
Del_A=Del_x(1:n_bus-1);
Del_V=Del_x(n_bus:end);
Delta(2:n_bus) = Del_A + Delta(2:n_bus);
x = 1;
for y = 2:n_bus
    if Type(y) == 2
        Vol(y) = Del_V(x) + Vol(y);
        x = x+1;
    end
end
end

Iteration = Iteration + 1;
lf=lf+0.25;
Tolerance_old = Tolerance;
Tolerance = max(abs(Del_PQ));
if(Tolerance > Tolerance_old)
    disp('Singular Point reached!!!')
    lf=lf_max+1;
    break;
end
end

```



```

end

Jr_QV = J4-J3*inv(J1)*J2;
Jr_PA = J1-J2*inv(J4)*J3;
[rev_QV, ev_QV] = eig(Jr_QV);
[lev_QV, ~] = eig(Jr_QV. ');
lev_QV = conj(lev_QV);
[rev_PA, ev_PA] = eig(Jr_PA);
[lev_PA, ~] = eig(Jr_PA. ');
lev_PA = conj(lev_PA);
Jn1 = ((J1+J1')/2);
Jn2 = ((J2+J3')/2);
Jn3 = ((J3+J2')/2);
Jn4 = ((J4+J4')/2);
Jr_nQV = Jn4-Jn3*inv(Jn1)*Jn2;
Jr_nPA = Jn1-Jn2*inv(Jn4)*Jn3;
[rev_nQV, ev_nQV] = eig(Jr_nQV);
[lev_nQV, ~] = eig(Jr_nQV. ');
lev_nQV = lev_nQV. ';
[rev_nPA, ev_nPA] = eig(Jr_nPA);
[lev_nPA, ~] = eig(Jr_nPA. ');
lev_nPA = lev_nPA. ';
e_QV=diag(ev_QV);
e_nQV=diag(ev_nQV);
e_PA=diag(ev_PA);
e_nPA=diag(ev_nPA);
sub_QV=e_QV-e_nQV;
sub_PA=e_PA-e_nPA;

%{
%Reactive Power Demand - Graphs
figure; %1
scatter(X1,sub_QV,'r');
hold on
plot(e_nQV,'m');
hold on
plot(e_QV);
hold on
hline(0,'r')
grid on;
title('Critical Modes -Reactive Power Demand');
legend('Comparision','Symmetric Component','Ordinary Jacobian');
xlabel('System Mode');
ylabel('Eigen Values');
%}

%{
%Active Power Demand - Graphs
figure; %2
scatter(X2,sub_PA,'r');
hold on
plot(e_nPA,'m');
hold on
plot(abs(e_PA));
hold on
hline(0,'g');

```

```

grid on;
title('Critical Modes - Active Power Demand');
legend('Comparision','Symmetric Component','Ordinary Jacobian');
xlabel('System Mode');
ylabel('Eigen Values');
%}

%Reactive Power Demand - Critical mode
%{
cm1_QV = cm;
cm2_QV = cm;
cm1_PA = cm;
cm2_PA = cm;
%}

[cm1_QV,~] = find(e_QV==min(e_QV));
%sub_QV(sub_QV==min(sub_QV)) = inf;
[cm2_QV,~] = find(e_nQV==min(e_nQV));
%Active Power Demand - Critical mode
[cm1_PA,~] = find(e_PA==min(e_PA));
%sub_PA(sub_PA==min(sub_PA)) = inf;
[cm2_PA,~] = find(e_nPA==min(e_nPA));

%Reactive Power Demand - Bus Participation Factors
bpf_rp1 = zeros(1,length(e_QV));
bpf_rp2 = zeros(1,length(e_QV));
bpf_rp3 = zeros(1,length(e_QV));
bpf_rp4 = zeros(1,length(e_QV));
for i=1:length(e_QV)
    bpf_rp1(1,i) = rev_QV(i,cm1_QV)*lev_QV(cm1_QV,i);
    bpf_rp2(1,i) = rev_nQV(i,cm1_QV)*lev_nQV(cm1_QV,i);
    bpf_rp3(1,i) = rev_QV(i,cm2_QV)*lev_QV(cm2_QV,i);
    bpf_rp4(1,i) = rev_nQV(i,cm2_QV)*lev_nQV(cm2_QV,i);
end

%{
figure;
%3
bpf_rp = [abs(bpf_rp1); abs(bpf_rp2); abs(bpf_rp3); abs(bpf_rp4)];
bar(bpf_rp','grouped');
title('Bus Participation Factor - Reactive Power Demand');
legend('Jo-Eo','Jo-Es','Js-Eo','Js-Es');
xlabel('Bus Number');
ylabel('Participation factor');
%}

%Active Power Demand - Bus Participation Factors
bpf_ap1 = zeros(1,length(e_PA));
bpf_ap2 = zeros(1,length(e_PA));
bpf_ap3 = zeros(1,length(e_PA));
bpf_ap4 = zeros(1,length(e_PA));
for i=1:length(e_PA)
    bpf_ap1(1,i) = rev_PA(i,cm1_PA)*lev_PA(cm1_PA,i);
    bpf_ap2(1,i) = rev_nPA(i,cm1_PA)*lev_nPA(cm1_PA,i);
    bpf_ap3(1,i) = rev_PA(i,cm2_PA)*lev_PA(cm2_PA,i);
    bpf_ap4(1,i) = rev_nPA(i,cm2_PA)*lev_nPA(cm2_PA,i);
end

```

```

%{
figure;
%4
bpf_ap = [abs(bpf_ap1); abs(bpf_ap2); abs(bpf_ap3); abs(bpf_ap4)];
bar(bpf_ap','grouped');
title('Bus Participation Factor - Active Power Demand');
legend('Jo-Eo','Jo-Es','Js-Eo','Js-Es');
xlabel('Bus Number');
ylabel('Participation factor');
%}
Vol_lf(1,q) = Vol(lbn,1);
Vol_lf1(1,q) = Vol(26,1);
apf1(1,q)= abs(bpf_ap1(1,lbn-1));
apf2(1,q)= abs(bpf_ap2(1,lbn-1));
apf3(1,q)= abs(bpf_ap3(1,lbn-1));
apf4(1,q)= abs(bpf_ap4(1,lbn-1));

apf11(1,q)= abs(bpf_ap1(1,25));
apf12(1,q)= abs(bpf_ap2(1,25));
apf13(1,q)= abs(bpf_ap3(1,25));
apf14(1,q)= abs(bpf_ap4(1,25));
q=q+1;
end
Vol_grad = gradient(Vol_lf(1:(length(Vol_lf)-1)));
str_vg = sprintf('Voltage Gradient at Bus %d: ',lbn);
disp(str_vg); disp(abs(sum(100*Vol_grad)));
figure;
subplot(2,2,1);
plot(apf1,'r');
hold on;
plot(apf4,'g');
str1 = sprintf('Bus %d response to Active Power Demand',lbn);
title(str1);
legend('Jo-Eo','Js-Es');
xlabel('Loading factor');
ylabel('Participation factor');
subplot(2,2,2);
plot(apf11,'r');
hold on;
plot(apf14,'g');
title('Bus 26 response to Active Power Demand');
legend('Jo-Eo','Js-Es');
xlabel('Loading factor');
ylabel('Participation factor');
subplot(2,2,3);
plot(Vol_lf(1:(length(Vol_lf)-1)))
str3 = sprintf('Voltage variation at bus %d', lbn);
title(str3);
xlabel('Loading Factor');
ylabel('Voltage');
subplot(2,2,4);
plot(Vol_lf1(1:(length(Vol_lf1)-1)));
title('Voltage Variation at Bus 26')
xlabel('Loading Factor');
ylabel('Voltage');

```

```

%{
figure;
subplot(1,2,1);
plot(apf2,'b');
hold on;
plot(apf3,'m');
str2 = sprintf('Alternate: Bus %d response to Active Power
Demand',lbn);
title(str2);
legend('Jo-Es','Js-Eo');
xlabel('Loading factor');
ylabel('Participation factor');
subplot(1,2,2);
plot(apf12,'b');
hold on;
plot(apf13,'m');
title('Alternate: Bus 26 response to Active Power Demand');
legend('Jo-Es','Js-Eo');
xlabel('Loading factor');
ylabel('Participation factor');
%}
%Solution(n_bus,Vol,Delta,line,lf,1);

end

```

Appendix C. Custom Load flow program – Critical Mode Identification

```

function[] = custom_load_flow_cm(busno,line,base)
ieee_bus=busno;
Ymatrix=ybus(ieee_bus,line);
switch busno
    case 4
    case 5
        data='IEEE5.xlsx';
    case 14
        data='IEEE14.xlsx';
    case 30
        data='IEEE30.xlsx';
    case 118
        data='IEEE118.xlsx';
end
base_MVA=base;
Type=xlsread(data,2,sprintf('B3:B%d',(2+ieee_bus)));
Pg=xlsread(data,2,sprintf('C3:C%d',(2+ieee_bus)));
Qg=xlsread(data,2,sprintf('D3:D%d',(2+ieee_bus)));
Pl=xlsread(data,2,sprintf('E3:E%d',(2+ieee_bus)));
Ql=xlsread(data,2,sprintf('F3:F%d',(2+ieee_bus)));
Vol=xlsread(data,2,sprintf('G3:G%d',(2+ieee_bus)));
Qmin=xlsread(data,2,sprintf('H3:H%d',(2+ieee_bus)));
Qmax=xlsread(data,2,sprintf('I3:I%d',(2+ieee_bus)));
Delta=xlsread(data,2,sprintf('J3:J%d',(2+ieee_bus)));
Pg=Pg/base_MVA;
Qg=Qg/base_MVA;

```

```

P1=P1/base_MVA;
Q1=Q1/base_MVA;
lf=1;
l=1;
P1=lf*P1;
Q1=l*Q1;
Qmin=Qmin/base_MVA;
Qmax=Qmax/base_MVA;
P=Pg-P1;
Q=Qg-Q1;
Pspec=P;
Qspec=Q;
G=real(Ymatrix);
B=imag(Ymatrix);
PV=find(Type==1 | Type==3); %PV
PQ=find(Type==2); %PQ
n_PV=length(PV);
n_PQ=length(PQ);
n_bus=length(Vol);
Tolerance=10000000;
Iteration=1;
tic;
while(Tolerance>0.0001)
    P = zeros(n_bus,1);
    Q = zeros(n_bus,1);

    for i = 1:n_bus
        for k = 1:n_bus
            P(i) = P(i) + Vol(i)* Vol(k)*(G(i,k)*cos(Delta(i)-Delta(k))
+ B(i,k)*sin(Delta(i)-Delta(k)));
            Q(i) = Q(i) + Vol(i)* Vol(k)*(G(i,k)*sin(Delta(i)-Delta(k))
- B(i,k)*cos(Delta(i)-Delta(k)));
        end
    end

    dPa = Pspec-P;
    dQa = Qspec-Q;
    k = 1;
    dQ = zeros(n_PQ,1);
    for i = 1:n_bus
        if Type(i) == 2
            dQ(k,1) = dQa(i);
            k = k+1;
        end
    end
    dP = dPa(2:n_bus);
    Del_PQ = [dP; dQ];

    J1 = zeros(n_bus-1,n_bus-1);
    for i = 1:(n_bus-1)
        k = i+1;
        for j = 1:(n_bus-1)
            m = j+1;
            if m == k
                for m = 1:n_bus

```

```

        J1(i,j) = J1(i,j) + Vol(k)* Vol(m)*(-
G(k,m)*sin(Delta(k)-Delta(m)) + B(k,m)*cos(Delta(k)-Delta(m)));
        end
        J1(i,j) = J1(i,j) - Vol(k)^2*B(k,k);
    else
        J1(i,j) = Vol(k)* Vol(m)*(G(k,m)*sin(Delta(k)-Delta(m))
- B(k,m)*cos(Delta(k)-Delta(m)));
    end
end
end
J2 = zeros(n_bus-1,n_PQ);
for i = 1:(n_bus-1)
    k = i+1;
    for j = 1:n_PQ
        m = PQ(j);
        if m == k
            for m = 1:n_bus
                J2(i,j) = J2(i,j) + Vol(m)*(G(k,m)*cos(Delta(k)-
Delta(m)) + B(k,m)*sin(Delta(k)-Delta(m)));
            end
            J2(i,j) = J2(i,j) + Vol(k)*G(k,k);
        else
            J2(i,j) = Vol(k)*(G(k,m)*cos(Delta(k)-Delta(m)) +
B(k,m)*sin(Delta(k)-Delta(m)));
        end
    end
end
J3 = zeros(n_PQ,n_bus-1);
for i = 1:(n_PQ)
    k = PQ(i);
    for j = 1:(n_bus-1)
        m = j+1;
        if m == k
            for m = 1:n_bus
                J3(i,j) = J3(i,j) + Vol(k)*
Vol(m)*(G(k,m)*cos(Delta(k)-Delta(m)) + B(k,m)*sin(Delta(k)-Delta(m)));
            end
            J3(i,j) = J3(i,j) - Vol(k)^2*G(k,k);
        else
            J3(i,j) = Vol(k)* Vol(m)*(-G(k,m)*cos(Delta(k)-
Delta(m)) - B(k,m)*sin(Delta(k)-Delta(m)));
        end
    end
end
J4 = zeros(n_PQ,n_PQ);
for i = 1:(n_PQ)
    k = PQ(i);
    for j = 1:n_PQ
        m = PQ(j);
        if m == k
            for m = 1:n_bus
                J4(i,j) = J4(i,j) + Vol(m)*(G(k,m)*sin(Delta(k)-
Delta(m)) - B(k,m)*cos(Delta(k)-Delta(m)));
            end
            J4(i,j) = J4(i,j) - Vol(k)*B(k,k);
        else

```

```

        J4(i,j) = Vol(k)*(G(k,m)*sin(Delta(k)-Delta(m)) -
B(k,m)*cos(Delta(k)-Delta(m)));
        end
    end
end
J=[J1 J2; J3 J4];
Del_x=J\Del_PQ;
Del_A=Del_x(1:n_bus-1);
Del_V=Del_x(n_bus:end);
Delta(2:n_bus) = Del_A + Delta(2:n_bus);
x = 1;
for y = 2:n_bus
    if Type(y) == 2
        Vol(y) = Del_V(x) + Vol(y);
        x = x+1;
    end
end

Iteration = Iteration + 1;
% lf=lf+0.25;
Tolerance_old = Tolerance;
Tolerance = max(abs(Del_PQ));
if(Tolerance > Tolerance_old)
    disp('Singular Point reached!!');
    break;
end
end

Jr_QV = J4-J3*inv(J1)*J2;
Jr_PA = J1-J2*inv(J4)*J3;
[rev_QV, ev_QV] = eig(Jr_QV);
[lev_QV, ~] = eig(Jr_QV. ');
lev_QV = conj(lev_QV);
[rev_PA, ev_PA] = eig(Jr_PA);
[lev_PA, ~] = eig(Jr_PA. ');
lev_PA = conj(lev_PA);
Jn1 = ((J1+J1')/2);
Jn2 = ((J2+J3')/2);
Jn3 = ((J3+J2')/2);
Jn4 = ((J4+J4')/2);
Jr_nQV = Jn4-Jn3*inv(Jn1)*Jn2;
Jr_nPA = Jn1-Jn2*inv(Jn4)*Jn3;
[rev_nQV, ev_nQV] = eig(Jr_nQV);
[lev_nQV, ~] = eig(Jr_nQV. ');
lev_nQV = lev_nQV. ';
[rev_nPA, ev_nPA] = eig(Jr_nPA);
[lev_nPA, ~] = eig(Jr_nPA. ');
lev_nPA = lev_nPA. ';
e_QV=diag(ev_QV);
e_nQV=diag(ev_nQV);
e_PA=diag(ev_PA);
e_nPA=diag(ev_nPA);
sub_QV=e_QV-e_nQV;
sub_PA=e_PA-e_nPA;
X1 = [1:length(sub_QV)];
X2 = [1:length(sub_PA)];

```

```

%Reactive Power Demand - Graphs
figure;
scatter(X1,sub_QV,'r');
hold on
plot(e_nQV,'m');
hold on
plot(e_QV);
hold on
hline(0,'r');
grid on;
title('Critical Modes - Reactive Power Demand');
legend('Comparision','Symmetric Component','Ordinary Jacobian');
xlabel('System Mode');
ylabel('Eigen Values');

%Active Power Demand - Graphs
figure;
scatter(X2,sub_PA,'r');
hold on
plot(e_nPA,'m');
hold on
plot(abs(e_PA));
hold on
hline(0,'g');
grid on;
title('Critical Modes - Active Power Demand');
legend('Comparision','Symmetric Component','Ordinary Jacobian');
xlabel('System Mode');
ylabel('Eigen Values');

%Reactive Power Demand - Critical mode
%{
cm1_QV = cm;
cm2_QV = cm;
cm1_PA = cm;
cm2_PA = cm;
%}
[cm1_QV,~] = find(e_QV==min(e_QV));
%sub_QV(sub_QV==min(sub_QV)) = inf;
[cm2_QV,~] = find(e_nQV==min(e_nQV));
%Active Power Demand - Critical mode
[cm1_PA,~] = find(e_PA==min(e_PA));
%sub_PA(sub_PA==min(sub_PA)) = inf;
[cm2_PA,~] = find(e_nPA==min(e_nPA));

%Reactive Power Demand - Bus Participation Factors
bpf_rp1 = zeros(1,length(e_QV));
bpf_rp2 = zeros(1,length(e_QV));
bpf_rp3 = zeros(1,length(e_QV));
bpf_rp4 = zeros(1,length(e_QV));
for i=1:length(e_QV)
    bpf_rp1(1,i) = rev_QV(i,cm1_QV)*lev_QV(cm1_QV,i);
    bpf_rp2(1,i) = rev_nQV(i,cm1_QV)*lev_nQV(cm1_QV,i);

```



```

    bpf_rp3(1,i) = rev_QV(i,cm2_QV)*lev_QV(cm2_QV,i);
    bpf_rp4(1,i) = rev_nQV(i,cm2_QV)*lev_nQV(cm2_QV,i);
end

figure;
%3
bpf_rp = [abs(bpf_rp1); abs(bpf_rp2); abs(bpf_rp3); abs(bpf_rp4)];
bar(bpf_rp','grouped');
title('Bus Participation Factor - Reactive Power Demand');
legend('Jo-Eo','Jo-Es','Js-Eo','Js-Es');
xlabel('Bus Number');
ylabel('Participation factor');

%Active Power Demand - Bus Participation Factors
bpf_ap1 = zeros(1,length(e_PA));
bpf_ap2 = zeros(1,length(e_PA));
bpf_ap3 = zeros(1,length(e_PA));
bpf_ap4 = zeros(1,length(e_PA));
for i=1:length(e_PA)
    bpf_ap1(1,i) = rev_PA(i,cm1_PA)*lev_PA(cm1_PA,i);
    bpf_ap2(1,i) = rev_nPA(i,cm1_PA)*lev_nPA(cm1_PA,i);
    bpf_ap3(1,i) = rev_PA(i,cm2_PA)*lev_PA(cm2_PA,i);
    bpf_ap4(1,i) = rev_nPA(i,cm2_PA)*lev_nPA(cm2_PA,i);
end

figure;
%4
bpf_ap = [abs(bpf_ap1); abs(bpf_ap2); abs(bpf_ap3); abs(bpf_ap4)];
bar(bpf_ap','grouped');
title('Bus Participation Factor - Active Power Demand');
legend('Jo-Eo','Jo-Es','Js-Eo','Js-Es');
xlabel('Bus Number');
ylabel('Participation factor');

Solution(n_bus,Vol,Delta,line,lf,1);

end

```

Appendix D. Solution and Results Program

```

function[] = Solution(n_bus,Vol,Delta,line,lf,1)

ieee_bus=n_bus;
ieee_line=line;
Y = ybus(ieee_bus,line);
Vm = Vol.*cos(Delta) + li*Vol.*sin(Delta);
Del = 180/pi*Delta;
switch n_bus
    case 5

```

```

        data='IEEE5.xlsx';
    case 14
        data='IEEE14.xlsx';
    case 30
        data='IEEE30.xlsx';
    case 118
        data='IEEE118.xlsx';
end
Type=xlsread(data,2,sprintf('B3:B%d',(2+ieee_bus)));
P1=xlsread(data,2,sprintf('E3:E%d',(2+ieee_bus)));
Q1=xlsread(data,2,sprintf('F3:F%d',(2+ieee_bus)));
P1=lf*P1;
Q1=1*Q1;
sb=xlsread(data,1,sprintf('A2:A%d',(1+ieee_line)));
eb=xlsread(data,1,sprintf('B2:B%d',(1+ieee_line)));
nl = length(sb);
Iij = zeros(n_bus,n_bus);
Sij = zeros(n_bus,n_bus);
Si = zeros(n_bus,1);
base_MVA=100;

I = Y*Vm;
Im = abs(I);
Ia = angle(I);

for m = 1:nl
    p = sb(m); q = eb(m);
    Iij(p,q) = -(Vm(p) - Vm(q))*Y(p,q);
    Iij(q,p) = -Iij(p,q);
end
Iij = sparse(Iij);
Iijm = abs(Iij);
Iija = angle(Iij);

for m = 1:n_bus
    for n = 1:n_bus
        if m ~= n
            Sij(m,n) = Vm(m)*conj(Iij(m,n))*base_MVA;
        end
    end
end
Sij = sparse(Sij);
Pij = real(Sij);
Qij = imag(Sij);

Lij = zeros(nl,1);
for m = 1:nl
    p = sb(m); q = eb(m);
    Lij(m) = Sij(p,q) + Sij(q,p);
end
Lpij = real(Lij);
Lqij = imag(Lij);

```

```

for i = 1:n_bus
    for k = 1:n_bus
        Si(i) = Si(i) + conj(Vm(i))* Vm(k)*Y(i,k)*base_MVA;
    end
end
Pi = real(Si);
Qi = -imag(Si);
Pg = Pi+Pl;
Qg = Qi+Ql;
n=[1:n_bus]';
xlswrite(data, n, 3, sprintf( 'A3:A%d', (2+n_bus)));
Total = [sum(Pi+Pl) sum(Qi+Ql) sum(Pl) sum(Ql)];
label = {'Total' ''};
soln = [Type RoundByRatCommand(Pg) RoundByRatCommand(Qg)
RoundByRatCommand(Pl) RoundByRatCommand(Ql) RoundByRatCommand(Vol)
RoundByRatCommand(Del)];
xlswrite(data, soln, 3, 'B3');
xlswrite(data, label, 3, sprintf( 'A%d', (4+n_bus)));
xlswrite(data, Total, 3, sprintf( 'C%d', (4+n_bus)));
Pse = zeros(nl,1);
Qse = zeros(nl,1);
Pes = zeros(nl,1);
Qes = zeros(nl,1);
for z=1:nl
    s=sb(z); e=eb(z);
    Pse(z,1) = Pij(s,e);
    Qse(z,1) = Qij(s,e);
    Pes(z,1) = Pij(e,s);
    Qes(z,1) = Qij(e,s);
end
lineflow = [sb eb Pse Qse eb sb Pes Qes Lpij Lqij];
xlswrite(data, lineflow, 4, 'A3');
winopen(data);

```

Appendix E. Jacobian Indices and Gerschgorin Circles

```

function[index1,index2,index3,index4] = Jacobian_Indices(J1,J2,J3,J4)
J=[J1 J2; J3 J4];
Js = 0.5*[J1+J1' J2+J3'; J3+J2' J4+J4'];
Jas = 0.5*[J1-J1' J2-J3'; J3-J2' J4-J4'];
[~,si_J,~]=svd(J);
[~,si_Js,~]=svd(Js);
[~,si_Jas,~]=svd(Jas);
J_SIN = diag(si_J);
Js_SIN = diag(si_Js);
Jas_SIN = diag(si_Jas);
Js_w = zeros(length(Js_SIN),1);
Jas_w = zeros(length(Jas_SIN),1);
Jn_w = zeros(length(J_SIN),1);
Jd_w = zeros(length(J_SIN),1);
Msig_Js = 0;
Msig_Jas = 0;
Msig_Jn = 0;

```

```

Msig_Jd = 0;
for i = 1:length(Js_SIN)
    Js_w(i)=Js_SIN(i)/sum(Js_SIN);
end
for i = 1:length(Jas_SIN)
    Jas_w(i)=Jas_SIN(i)/sum(Jas_SIN);
end
for i = 1:length(J_SIN)
    Jn_w(i)=(J_SIN(i)-Js_SIN(i))/sum(J_SIN-Js_SIN);
end
for i = 1:length(J_SIN)
    Jd_w(i)=(J_SIN(i)-Jas_SIN(i))/sum(J_SIN-Jas_SIN);
end
for i = 1:length(Js_SIN)
    Msig_Jn = Msig_Jn + Jn_w(i)*(J_SIN(i)-Js_SIN(i));
end
for i = 1:length(Js_SIN)
    Msig_Jd = Msig_Jd + Jd_w(i)*(J_SIN(i)-Jas_SIN(i));
end
for i = 1:length(Js_SIN)
    Msig_Js = Msig_Js + Js_w(i)*Js_SIN(i);
end
for i = 1:length(Jas_SIN)
    Msig_Jas = Msig_Jas + Jas_w(i)*Jas_SIN(i);
end

index1 = Msig_Jas/Msig_Js;
index2 = norm(Jas_SIN,2)/norm(Js_SIN,2);
index3 = norm(Jas_SIN,'fro')/norm(Js_SIN,'fro');
index4 = 3*(Msig_Jn/Msig_Jd);

[r_J1,c_J1] = size(J1);
radii_J1=zeros(r_J1,1);
for i = 1:r_J1
    for j = 1:c_J1
        if i~=j
            radii_J1(i,1)= radii_J1(i,1)+norm(((J1(i,j)+J1(j,i))/2),2);
        end
    end
end
centre_J1 = diag(J1);
[~, eigv_J1s] = eig((J1+J1')/2);
nzc(radii_J1);
nzc(eigv_J1s);
[~, eigv_J1d] = eig((J1-J1')/2);
figure;
for c = 1:r_J1
    circle(centre_J1(c,1),0,radii_J1(c,1));
    hold on;
end
[~,~,eigv_J1s] = find(sparse(eigv_J1s));
[~,~,eigv_J1d] = find(sparse(eigv_J1d));
scatter(eigv_J1s,zeros(c_J1,1))
hold on;
scatter(zeros(length(imag(eigv_J1d)),1),imag(eigv_J1d))

```

```

[r_J4,c_J4] = size(J4);
radii_J4=zeros(r_J4,1);
for i = 1:r_J4
    for j = 1:c_J4
        if i~=j
            radii_J4(i,1)= radii_J4(i,1)+norm(((J4(i,j)+J4(j,i))/2),2);
        end
    end
end
centre_J4 = diag(J4);
[~, eigv_J4s] = eig((J4+J4')/2);
nnz(radii_J4);
nnz(eigv_J4s);
[~, eigv_J4d] = eig((J4-J4')/2);
figure;
for c = 1:r_J4
    circle(centre_J4(c,1),0,radii_J4(c,1));
    hold on;
end
[~,~,eigv_J4s] = find(sparse(eigv_J4s));
[~,~,eigv_J4d] = find(sparse(eigv_J4d));
scatter(eigv_J4s,zeros(c_J4,1))
hold on;
scatter(zeros(length(imag(eigv_J4d)),1),imag(eigv_J4d))

[r_J,c_J] = size(J);
radii_J=zeros(r_J,1);
for i = 1:r_J
    for j = 1:c_J
        if i~=j
            radii_J(i,1)= radii_J(i,1)+norm(((J(i,j)+J(j,i))/2),2);
        end
    end
end
centre_J = diag(J);
[~, eigv_Js] = eig((J+J')/2);
nnz(radii_J);
nnz(eigv_Js);
[~, eigv_Jd] = eig((J-J')/2);
figure;
for c = 1:r_J
    circle(centre_J(c,1),0,radii_J(c,1));
    hold on;
end
[~,~,eigv_Js] = find(sparse(eigv_Js));
[~,~,eigv_Jd] = find(sparse(eigv_Jd));
scatter(eigv_Js,zeros(c_J,1))
hold on;
scatter(zeros(length(imag(eigv_Jd)),1),imag(eigv_Jd))
end

```